J. Membrane Biol. 129, 13–36 (1992)

The Journal of
Membrane Biology

Cell Swelling Activates K^+ and Cl^- Channels as well as Nonselective, Stretch-Activated Cation Channels in Ehrlich Ascites Tumor Cells

Ove Christensen† and E.K. Hoffmann‡

†Institute of General Physiology and Biophysics, Panum Institute, University of Copenhagen, DK-2200 Copenhagen N, Denmark, and ‡Institute of Biological Chemistry A, August Krogh Institute, University of Copenhagen, DK-2100 Copenhagen Ø, Denmark

Summary. Cell-attached patch-clamp recordings from Ehrlich ascites tumor cells reveal nonselective cation channels which are activated by mechanical deformation of the membrane. These channels are seen when suction is applied to the patch pipette or after osmotic cell swelling. The channel activation does not occur instantaneously but within a time delay of ½ to 1 min. The channel is permeable to Ba^{2+} and hence presumably to Ca^{2+}. It seems likely that the function of the nonselective, stretch-activated channels is correlated with their inferred Ca^{2+} permeability, as part of the volume-activated signal system. In isolated inside-out patches a Ca^{2+}-dependent, inwardly rectifying K^+ channel is demonstrated. The single-channel conductance recorded with symmetrical 150 mM K^+ solutions is for inward current estimated at 40 pS and for outward current at 15 pS. Activation of the K^+ channel takes place after an increase in Ca^{2+} from 10^{-7} to 10^{-6} M which is in the physiological range. Patch-clamp studies in cell-attached mode show K^+ channels with spontaneous activity and with characteristics similar to those of the K^+ channel seen in excised patches. The single-channel conductance for outward current at 5 mM external K^+ is estimated at about 7 pS. A K^+ channel with similar properties can be activated in the cell-attached mode by addition of Ca^{2+} plus ionophore A23187. The channel is also activated by cell swelling, within 1 min following hypotonic exposure. No evidence was found of channel activation by membrane stretch (suction). The time-averaged number of open K^+ channels during regulatory volume decrease (RVD) can be estimated at 40 per cell. The number of open K^+ channels following addition of Ca^{2+} plus ionophore A23187 was estimated at 250 per cell. Concurrent activation in cell-attached patches of stretch-activated, nonselective cation channels and K^+ channels in the presence of 3 mM Ca^{2+} in the pipette suggests a close spatial relationship between the two channels. In excised inside-out patches (with NMDG chloride on both sides) a small 5-pS chloride channel with low spontaneous activity is observed. The channel activity was not dependent on Ca^{2+} and could not be activated by membrane stretch (suction). In cell-attached mode single-channel currents with characteristics similar to the channels seen in isolated patches are seen. In contrast to the channels seen in isolated patches, the channels in the cell-attached mode could be activated by addition of Ca^{2+} plus ionophore A23187. The channel is also activated by hypotonic exposure with a single-channel conductance at 7 pS (or less) and with a time delay at about 1 min. The number of open channels during RVD is estimated at 80 per cell. Two other types of Cl^- channels were regularly recorded in excised inside-out patches: a voltage-activated 400-pS channel and a 34-pS Cl^- channel which show properties similar to the Cl^- channel in the apical membrane in human airway epithelial cells. There is no evidence for a role in RVD for either of these two channels.

Key Words K^+ channel · Cl^- channel · patch clamp · nonselective cation channel · stretch-activated channel · volume regulation

Introduction

Volume regulation is a feature common to many vertebrate cells (for references, *see* recent reviews by Hoffmann & Simonsen, 1989; Okada & Hazama, 1989; Schultz, 1989; Chamberlin & Strange, 1990; Lewis & Donaldson, 1990; Hoffmann & Kolb, 1991; Spring & Hoffmann, 1991; Hoffmann & Ussing, 1992). When placed in a hypotonic bathing solution, these cells initially swell, but then, over several minutes, shrink back to near their resting volume. The regulatory volume decrease (RVD) is usually accompanied by the loss of intracellular K^+ and anions, mainly Cl^-. Several transport mechanisms have been proposed to be activated during RVD (*see* Hoffmann & Simonsen, 1989). Activation by cell swelling of separate, conductive K^+ and Cl^- transport pathways in single cells was first proposed for Ehrlich ascites tumor cells (Hoffmann, 1978). This notion has been confirmed in later studies of RVD in Ehrlich cells (*see* Hoffmann, Lambert & Simonsen, 1988) as well as in many other vertebrate cells (*see* Hoffmann & Simonsen, 1989). Activation of ion channels in hypotonically swollen Ehrlich cells has been directly demonstrated in studies using the patch-clamp technique (Hudson & Schultz, 1988).

The mechanism of volume-induced activation of the K^+ and Cl^- channels is only partly understood, but Ca^{2+} seems to be involved in the RVD response

in most cell types investigated (for a recent review *see* Pierce & Politis, 1990). In Ehrlich cells both Ca^{2+} entry and Ca^{2+} release from intracellular stores has been reported to play a role in the RVD response (*see* Hoffmann et al., 1988; Hoffmann & Simonsen, 1989). An increase in $[Ca^{2+}]_i$ could directly activate a Ca^{2+}-activated K^+ channel. The role of $[Ca^{2+}]_i$ in the activation of the Cl^- channel has been proposed to be indirect and mediated via Ca^{2+}-induced stimulation of leukotriene synthesis (*see* Hoffmann et al., 1988).

The nature of the sensory mechanisms detecting the volume changes during RVD is, as yet, totally unknown. Over the last couple of years, however, stretch-activated, cation-selective ion channels, which appear to be ubiquitous (Guharay & Sachs, 1984; Christensen, 1987; Lansman, Hallam & Rink, 1987; Kirber, Walsh & Singer, 1988; Falke & Misler, 1989; Sackin, 1989; Hoffmann & Kolb, 1991) have been proposed as a possible candidate for the "sensor" mechanisms in cell volume regulation. The stretch-activated channel reported by Sackin (1989) in the basolateral membrane of *Necturus* proximal tubules is K^+ selective, in contrast to the stretch-activated cation channels in most other cell types which have been found to be cation nonspecific. The channels are in general permeable to Ca^{2+} and may allow sufficient Ca^{2+} to enter to serve a second messenger function (Christensen, 1987; Lansman et al., 1987).

In the present report we demonstrate nonselective cation channels in Ehrlich cells which can be activated either after osmotic cell swelling or by mechanical stress (suction). The channel conducts Ba^{2+}, an often used indication of Ca^{2+} conductance. The activity of the stretch-activated, nonselective cation channels increases shortly after the onset of osmotically induced cell swelling and gradually decreases during RVD.

The present study also reports patch-clamp studies to characterize the K^+ and Cl^- channels activated by cell swelling in Ehrlich cells. The volume-activated Cl^- channel is small with a single-channel conductance of 2 to 7 pS. In inside-out patches the Cl^- channel cannot be activated by Ca^{2+}. The volume-activated K^+ channel is a Ca^{2+}-activated inward-rectifier channel with 40-pS conductance for inward currents and 15 pS for outward currents, similar to the small, Ca^{2+}-activated K^+ channel in red cells (Grygorczyk, Schwarz & Passow, 1984) and HeLa cells (Sauvé et al., 1986, 1988). In inside-out patches neither of the channels are stretch activated. In cell-attached patches both the K^+ and the Cl^- channel are fully activated by hypotonic cell swelling and by addition of the Ca^{2+} ionophore A23187. The activation of the Cl^- channel after hypotonic exposure is delayed about 30–50 sec.

It seems likely that the function of the stretch-activated, nonselective cation channels is correlated with their putative Ca^{2+} permeability. In combination with Ca^{2+} release from internal stores this could produce an increase in $[Ca^{2+}]_i$ which could in turn directly or indirectly activate the K^+ and Cl^- channels which are not directly activated by mechanical stress. A significant cell depolarization during RVD has been observed in Ehrlich cells (*see* Hoffmann & Kolb, 1991) and may play a role in K^+ channel activation as proposed in other cell types (for references *see* Hoffmann & Simonsen, 1989; Rotin et al., 1991); such depolarization will be enhanced by the activation of stretch-activated, nonselective cation channels. Part of this work has been published previously in abstract form (Jakobsen, Christensen & Hoffmann, 1989). In inside-out patches neither of the channels are stretch activated. In cell-attached patches both the K^+ and the Cl^- channel are fully activated by hypotonic cell swelling and by addition of the Ca^{2+} ionophore A23187. The activation of the Cl^- channel after hypotonic exposure is delayed about 30–50 sec.

Materials and Methods

Cell Suspensions

Ehrlich mouse ascites tumor (EAT) cells (hyperdiploid strain) were maintained in the peritoneal cavity of white female Theiler mice by weekly transplantation and harvested eight days after transplantation. The ascites fluid was diluted in a standard salt solution (*see below*) containing heparin (2.5 IU/ml), and centrifuged (700 × *g*, 45 sec). The packed cells were resuspended and washed twice by centrifugation, once with the standard salt solution and once with the standard incubation medium (*see below*). The cells were finally resuspended in standard incubation medium, the cytocrit adjusted to 1% and the cell suspension incubated in a shaking bath at 37°C.

All experiments were performed at room temperature. Control experiments show that Ehrlich cells undergo RVD at this temperature at a rate of about three times lower than that previously described at 37°C (*see* Hoffmann, Lambert & Simonsen, 1986).

Solutions

The *standard incubation medium* was a RPMI-1640 medium (Biochrom KG) supplemented with salts to obtain final concentrations (in mM) of: NaCl 143, KCl 5, $CaCl_2$ 1, $MgSO_4$ 1, NaH_2PO_4 1, and with TES (N-tris-(hydroxymethyl)methyl-2-amino-ethane sulfonic acid) 3.3, and Tris (tris(hydroxymethylaminomethane)) 8.0. The final osmolality was 323 mOsm. *Standard salt solution* had the same salts and buffers as the standard incubation medium and nothing else. *Hypotonic incubation medium* was prepared by

diluting the isotonic standard incubation medium with one volume of a solution of TES and Tris in distilled water in concentrations as above (pH 7.4). Medium used with the Ca^{2+} ionophore A23187 had $CaCl_2$ reduced to 0.15 mM and $MgSO_4$ reduced to 0.01 mM. *Electrode solutions* (*see below*) contained 150 mM NaCl, KCl or N-methyl-D-glucamineCl (NMDGCl). All solutions were buffered by 8 mM Tris and 3.3 mM TES and pH was adjusted to 7.4. The ionophore A23187 was administered in a concentration of 10 μM in a solution with 20 μM albumin (1.34 mg/ml) as a carrier. This produces about 2 μM free ionophore (L.O. Simonsen, *personal communication*). K solutions buffered to different Ca^{2+} concentrations were made as described elsewhere (Christensen & Zeuthen, 1987).

Patch-Clamp Technique

The patch-clamp recordings were carried out essentially according to the method of Neher and Sakmann as described by Hamill et al. (1981) using the "cell-attached" and the "inside-out" configurations. Electrodes were pulled from borosilicate glass capillary tubes typically having a resistance of 5 MΩ when filled with 150-mM NaCl solution. They were covered by Sylgard® to reduce the current noise. Enzymatic cleaning of the cells was not necessary to obtain giga-seals.

EAT cells seal to the electrode quite easily. It is in most cases not possible to rupture the patch by suction. This makes it difficult to form the whole-cell configuration on these cells. Inside-out patches were formed directly from the cell-attached patches since vesicles at the electrode tip were not formed.

The current signal was digitized and recorded on a video recorder using a SONY PCM-701 ES converter modified to record DC signals. Most examples on single-channel currents shown here were played back from tape and filtered at 1 kHz (3 dB; 24 dB/octave; Bessel response) if not otherwise stated.

Electrical current is positive (upward deflections) when directed outward from the cell into the electrode (cell-attached patch) or from the bath into the electrode (inside-out patches). In our set-up, bath voltage was changed and the interior of the patch electrode was always nominally at zero voltage. This is in contrast to the basic circuit described by Hamill et al. (1981). Thus, the bath voltage used in the present investigation is equal to the negative value of the electrode holding voltage. The potential of the membrane patch (V_p) in a cell-attached patch equals the bath voltage (V_b) plus the (negative) cell membrane potential (V_m), i.e.:

$$V_p = V_b + V_m. \tag{1}$$

The current reversal potential (V_{rev}) is the value of bath voltage where the single-channel current changes sign. At this voltage the patch membrane potential equals the weighted sum of the equilibrium potentials (E_i) for the ion(s) passing through the channels of the patch ($\Sigma t_i E_i$) where the weighting factor $t_i = g_i/\Sigma g_i$ and g_i is the conductance of the ion. Thus, using Eq. (1) we get

$$V_{rev} = \Sigma t_i E_i - V_m. \tag{2}$$

Experimental Chamber

The experimental chamber was a modified version of the chamber described earlier (Christensen, Simon & Randlev, 1989). The time required to change solutions was measured using a TMA-selective electrode and TMA solutions with various concentrations. Solution change took place with an initial time lag of 10 sec followed by a mixing phase with a half time of 10 sec.

How to Distinguish between Different Channels in Cell-Attached Patches

In this work we will describe three different types of channel: a K^+ channel, a stretch-activated cation channel and a Cl^- channel. Often we see several channels in one patch. In order to be able to distinguish between these channels when they are activated in cell-attached patches, we have used different electrolytes in the electrode. We refer to zero and negative bath voltages. (i) With NMDGCL in the electrode, K^+ can only move outwards, which gives a positive patch current. The calculated Cl^- equilibrium potential will be less negative than the membrane potential (*see* Table 1), resulting also in outward movements of Cl^-, giving a negative patch current. Outward movements of K^+ and Na^+ through the nonspecific cation channel also give a positive current, but this turns out to be too small to be observed at normal to hyperpolarizing patch potentials. The Cl^- channel is here unambiguously defined. (ii) With NaCl in the electrode the only change is that Na^+ moves inwards through the cation channel, creating a negative current. This may sometimes obscure the Cl^- current, but in this situation, the K^+ current is unambiguously determined as the sole positive current. The cation channel is usually easy to distinguish from the small Cl^- channel because the conductance of the cation channel is much larger than that of the Cl^- channel. (iii) With KCl in the electrode V_p is more negative (at zero or negative bath voltage) than the equilibrium potential for any of the ions and all channel openings lead to negative currents. The K^+ and the cation channel are dominant here because of their larger conductance, and it is only possible to distinguish between these channels because of their different gating behaviors. Nevertheless, this situation gives larger K^+ unitary current amplitudes and was used in many cases.

Results

Nonselective Cation Channel: Cell-Attached Patches

Conductance and Reversal Potential

Figure 1 shows typical data for spontaneously active cation channels in cell-attached patches. Positive single-channel currents correspond to an outward movement of cations from the cell into the electrode. Conductance data for this channel type was obtained on 30 patches. In 11 of these, the electrode contained 150 mM NaCl. In 19 other patches with 150 mM KCl in the electrode (*not shown*) we have seen channels with similar characteristics. The channel is therefore a cation channel selective both for Na^+ and K^+. At the bottom panel of Fig. 1 it is demonstrated that negative single-channel currents can be obtained also with Ba^{2+} in the electrode, indicating that the Ba^{2+} can pass through the channel.

Table 1. Expected reversal potentials for channels in cell-attached patches

Type of channel Electrode contents (mM)	K^+ 150 K^+	Cl^- 150 Cl^-	Nonselective cation 150 Na^+ or K^+
Reference situation			
Internal concentration (mM)[a]	187.7 ± 3.2(46)	64.8 ± 2.6(44)	210.0 ± 4.3(37)
Equilibrium potential (mV)[b]	−5.7 ± 0.1(46)	−21.26 ± 0.9(44)	−8.5 ± 0.2(37)
Measured V_{rev} (mV)	49 ± 5(1)	25	34 ± 3(30)
Estimated V_{rev} with $V_c = -61$[c]	55.3	39	52.5
Estimated V_{rev} with $V_c = -57$[c]	51.3	35	48.5
Calculated V_m (mV)	−55 ± 5.1(11)	−45	−43 ± 3.2(30)
Hypotonically swollen cells			
Internal concentration (mM)[a]	93.9	32.4	105
Equilibrium potential (mV)	11.9	−38.8	9
Measured V_{rev} (mV)	60 ± 4(4)	—	54 ± 3(10)
Estimated V_{rev} with $V_c = -41$[c]	52.8	2.2	50
Calculated V_m (mV)	−48(4)	—	−45(10)

[a] Calculated as a mean of all separate experiments included in Hoffmann, Simonsen & Sjøholm (1979); Hoffmann, Lambert & Simonsen (1986); Kramhøft et al. (1986), and Lambert et al. (1989). In hypotonically swollen cells the internal concentrations are given at half the value in isotonic medium as Ehrlich cells behave initially as perfect osmometers (Hoffmann et al., 1984).

[b] $E = z \cdot 25.3 \cdot \ln(C_o/C_i)$; where C_o and C_i are the external and the internal concentrations, respectively, and z the charge number of the ion. The temperature was 21°C.

[c] Gstein et al. (1987) report $V_c = -57$ mV at 37°C. Lambert et al. (1989) report $V_c = -61$ mV in reference situation and $V_c = -41$ mV in hypotonic solution (at 37°C). Values are given as mean ± SEM with the number of independent experiments in parentheses.

The slope of the *I-V* curve is usually larger at negative voltages than at positive voltages. The slope measured in the typical range of 0 to 40 mV gives a channel conductance of 23.0 ± 1.2 pS (SEM, $n = 30$). The mean current reversal voltage (V_{rev}) was 34.0 ± 2.6 mV (SEM, $n = 30$). Values of V_{rev} obtained with KCl in the electrode were not significantly different from values obtained with NaCl in the electrode, indicating a selectivity ratio Na : K of unity. With 150 mM NMDGCl in the electrode, this channel was not seen. Thus the channel is not permeable to the large cation $NMDG^+$.

At the reversal potential the patch membrane potential equals the weighted sum of the equilibrium potentials for the cations across the patch. The internal cation concentration in the cell amounts to 210.0 mM (187.7 mM from K^+ and 22.3 mM from Na^+ ions) (*see* Table 1). Relative to the 150-mM Na^+ and K^+ in the electrode, this produces an equilibrium potential for the sum of the cation of −8.5 mV provided that Na^+ and K^+ conductances are identical. Since the current reversal voltage (V_{rev}) equals 34 mV, the expected cell potential is calculated at −9 + −34 mV = −43 mV using Eq. (2). This can be compared to a cell potential of −56 mV, as measured in Ehrlich cells by microelectrode (Gstrein, Paulmichl & Lang, 1987) and to −61 mV measured by a potential-sensitive fluorescent probe (Lambert, Hoffmann & Jørgensen, 1989). It should be noted that these membrane potentials are both measured at 37°C, whereas the patch-clamp experiments are carried out at room temperature.

We were particularly interested in whether the nonselective cation channel conducts Ca^{2+} because it then may let Ca^{2+} into the cell when the cell volume is changed. With 90 mM $CaCl_2$ in the electrode, we observed in most patches spike-like currents having little resemblance to unitary current events. In a single patch, we have seen unitary current events of very low activity in an otherwise inactive patch, indicating Ca^{2+} passage through this channel. External Ca^{2+} at high concentrations has been reported to result in very short channel openings in other nonselective cation channels (Moody & Bosma, 1989). Due to the technical difficulties encountered, we used Ba^{2+} as a substitute for Ca^{2+}. With Ba^{2+} in the electrode, we observed single-channel currents due to passage of Ba^{2+} through the channel, *see* Fig. 1, bottom panel. The conductance with 100 mM $BaCl_2$ in the electrode was 15–17 pS (three patches).

Gating Behavior for Spontaneously Active Nonspecific Cation Channels in the Cell-Attached Mode

The current traces in Fig. 2 show typical single-channel currents in spontaneously active channels. In trace *A* of the figure is shown the most common gating behavior (22 of 30 patches). In the open state

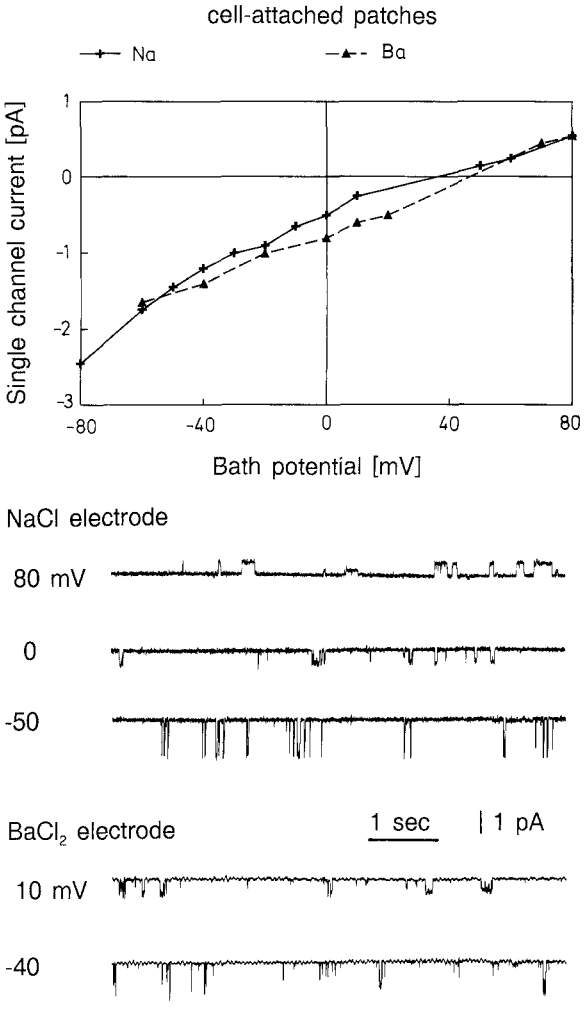

Fig. 1. Spontaneous single-channel current *versus* bath voltage for the nonselective cation channel in cell-attached patches. Data are shown with the electrode containing 150 mM NaCl (+) and 100 mM $BaCl_2$ (▲). The middle and bottom panels show typical current traces. The data shown with the electrode containing 150 mM NaCl are typical for 11 separate experiments; the data shown with $BaCl_2$ in the electrode are typical for 3 separate experiments. Low-pass filtered with 600-Hz bandwidth.

the single-channel current fluctuates. In a few patches (trace *B*), those fluctuations appear more like brief transitions to the channel closed state, giving a burst-like gating behavior. Often channel openings are seen with different current amplitudes from one channel opening to another (trace *C*). This may be due to discrete substates. In spontaneously active patches displaying the kinetic behavior shown in traces *A* and *B*, the open probability was low, typically 0.01. In the two traces in *D* of Fig. 2 are shown a gating mode with channel openings which last typically 1 to 10 sec and in some cases up to minutes. The current fluctuates vigorously. This gating behavior was observed in 9 of 30 patches. The open probability is much higher, about 0.1–0.6 evaluated over periods of minutes. In one patch, the normal as well as the noisy kinetic forms were observed simultaneously. Both gating modes occasionally show a behavior (Fig. 2, traces *E* and *F*) where the channel current changes almost continuously between the typical open channel current and zero current in the closed state. Histograms of current amplitude had Gaussian shape when averaged over many unitary single-channel current events. The three openings shown in the two *D* traces of Fig. 2 all had Gaussian-shaped amplitude histograms but with different position of the mean, i.e., current amplitude.

Stretch Activation of the Channel

The nonselective channel discussed above is activated by membrane stretch. In Fig. 3, upper panel, this is illustrated for a cell-attached patch. The stretch is produced by electrode suction to different negative pressures. The figure shows an example where the channel open probability initially was zero and gradually increases with increasing suction. The increase in channel open probability appears mainly to be due to increase of channel open time with increasing suction. Stretch activation by electrode suction could be performed only in about 30% of all cell-attached patches. This should be compared with the 50% activation by the hypotonic cell swelling.

Figure 3, bottom panel, shows stretch activation of cation channels in an inside-out patch with NMDGCl in the electrode. Only in 23 inside-out patches out of around 60 did we find stretch activation of channel activity produced by pipette suction.

Figure 4 demonstrates two phenomena, which may explain the failure to stretch activate channels in some patches. The first is the phenomenon of *desensitization* shown in Figure 4*A*. Upon repeatedly changing the "suction" to study stretch activation, we found that, at some point, the channel activity did not respond to changes in "suction" any more (activity did not turn off going to 0 cm in third trace), the channel was now permanently at a higher open probability. This might explain why channel activity could not be changed by electrode suction in many spontaneously active patches. In other patches, we have observed the *adaptation* phenomenon shown in Fig. 4*B*: the initially induced channel activity disappears before electrode suction is relieved. In these cases, further attempts to induce activity required a more negative electrode pressure (increased suction) if at all possible.

The absence of stretch activation may therefore

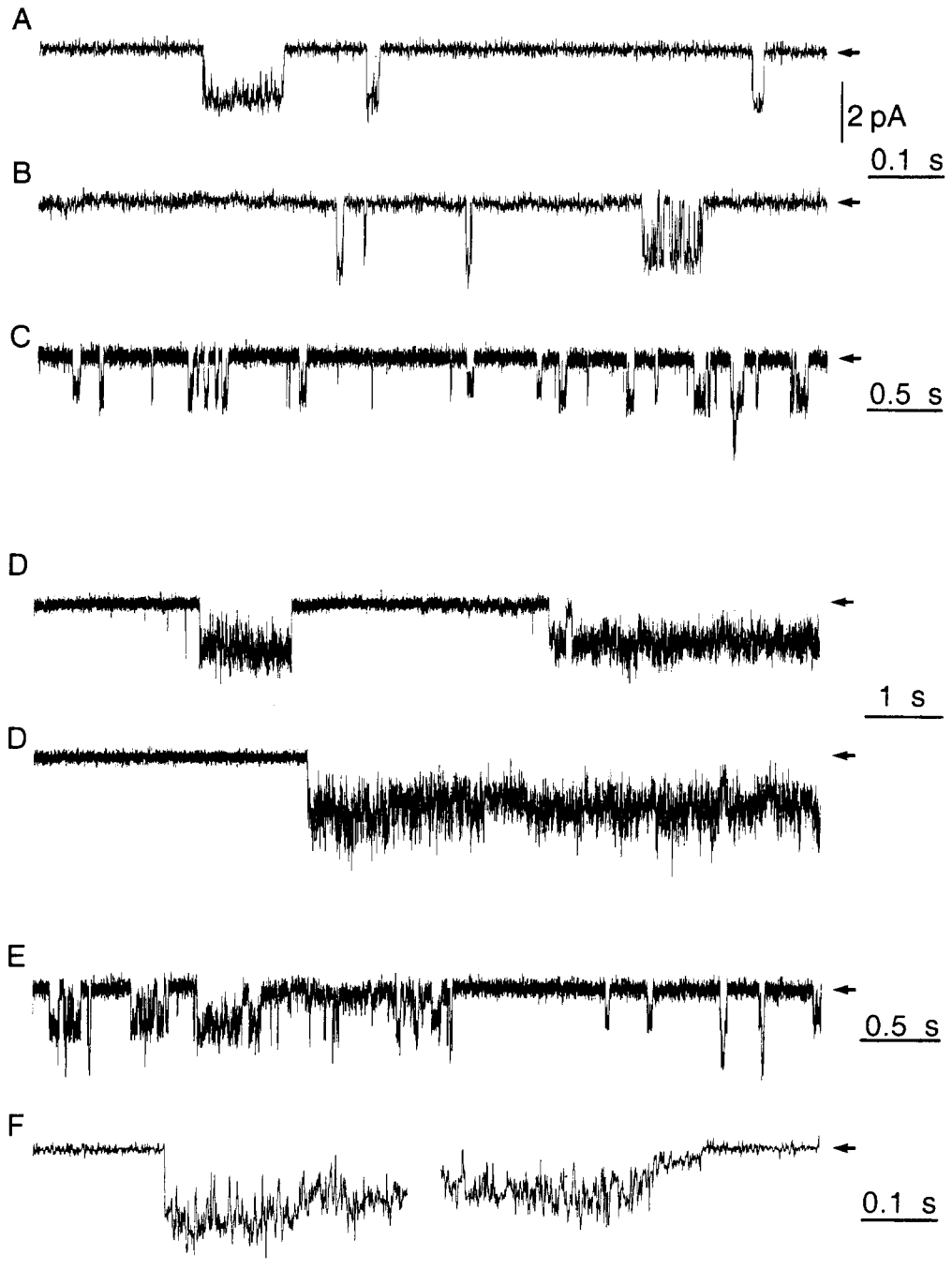

Fig. 2. Examples of the kinetic behavior of the SA channel in cell-attached patches obtained at 0- to −20-mV bath voltage and with 150 mM NaCl in the electrode. Trace *A*: The most commonly observed gating behavior. During channel openings, the current amplitude fluctuates in a noise-like manner. Trace *B*: In some cases, the current amplitude in the open state fluctuates so much that fluctuations appear to be fast closures, giving a burst-like gating behavior. Trace *C*: The spontaneous variation in single-channel current amplitude from one channel opening to the next. Trace *D*: Typical examples of channel current in the gating mode with long (> seconds) openings with vigorously fluctuating amplitude. The two traces in *D* show three openings at the same voltage. Trace *E*: An example of incomplete channel opening (or channel closure), appearing as a noisy baseline. Trace *F*: The opening and closing of a channel in the long bursting mode (*cf.* trade *D*). Notice the almost continuous transition to the channel closed state.

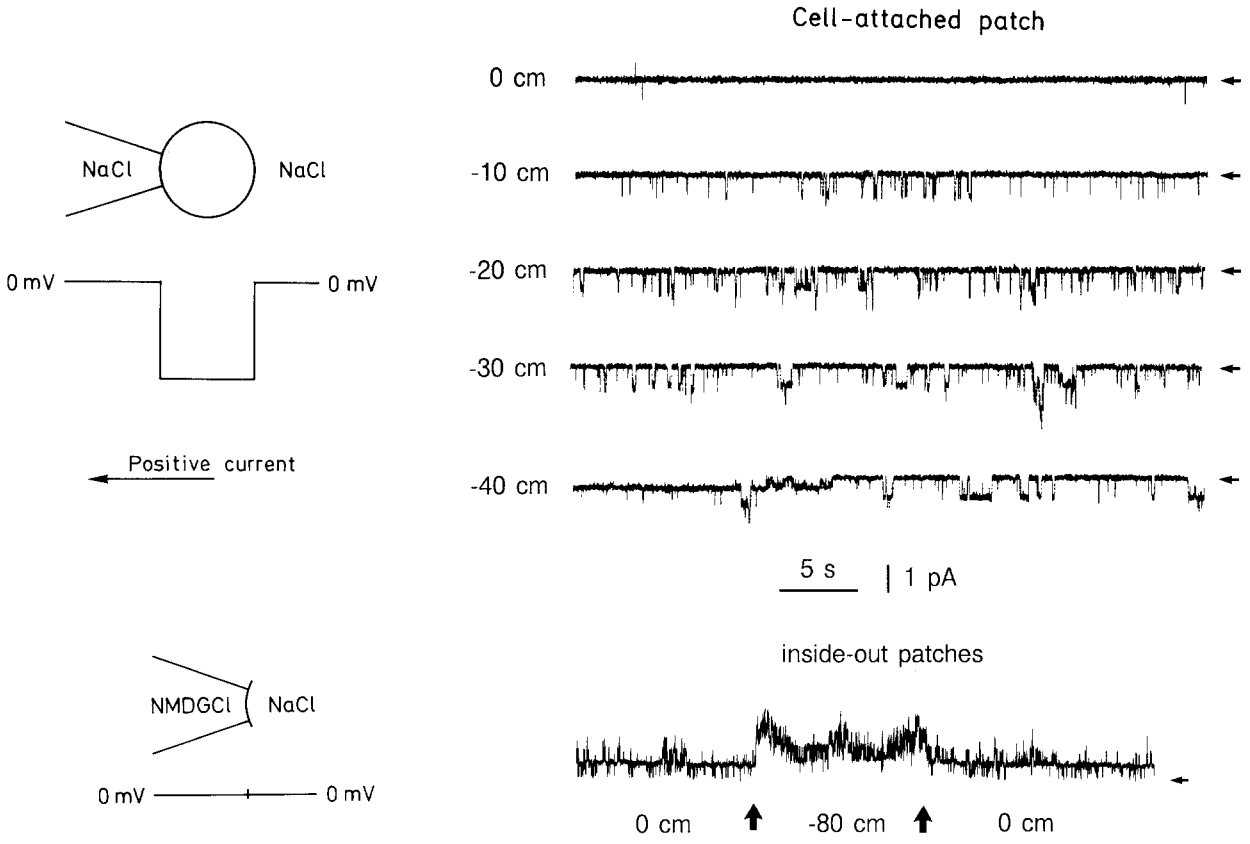

Fig. 3. Stretch-activation of the cation channel produced by pipette suction. The upper panel shows current recordings from an attached patch. The numbers on the left indicate the electrode pressure (cm H_2O), negative numbers indicate suction. Recordings obtained with NaCl in the electrode at 0-mV bath voltage. Notice the substate at −40 cm water pressure. The current trace at the bottom of the figure shows stretch activation of cation channels in an inside-out patch with NMDGCl in the electrode and NaCl in the bath. Horizontal arrows indicate baseline. Vertical arrows indicate change of pipette suction.

be due to the initial phases of giga-seal formation where part of the cell is deformed and pulled into the electrode by low electrode pressure. The possible desensitization or adaptation during this phase could be responsible for the failure to induce further activity in some patches.

The Stretch-Activated (SA) Cation Channel: Inside-Out Patches

In excised patches, the nonselective cation channel had a much higher spontaneous open probability (about 0.5) than in cell-attached patches. Furthermore, the single-channel currents showed usually 'well-behaved' unitary single-channel events with long (seconds) open and closed times rather than the more flickering behavior in cell-attached patches. In Fig. 5 are shown *I-V* curves for this channel under different conditions. The *I-V* curve is linear in symmetrical solutions of 150 mM NaCl (squares) with a conductance of 24.3 ± 1.6 pS (SEM, n = 6). When Na^+ is replaced by the impermeant ion $NMDG^+$ in the electrode (circles) or in the bath (triangles), single-channel currents are observed which go from the bath to the pipette (positive current) or from the pipette to the bath, respectively, at both positive and negative patch potentials. This indicates that the selectivity is much larger for Na^+ than for Cl^-.

With NMDGCl in the electrode the current was the same with Na^+, Li^+ or K^+ in the bath (K^+ channel activity was avoided by using a Ca^{2+}-free solution). Thus the selectivity ratio is $P_K : P_{Na} : P_{Li} = 1$. With Ba^{2+} in the electrode (crosses), the current is reduced to about 60% of the one obtained with Na^+, giving a conductance of 15 pS. With 90 mM Ca^{2+} on the inside, no channel activity was seen and activity did not immediately return when the bath medium was returned to NaCl. Internal Ca^{2+} was not necessary for channel activity.

We have not found any blockers for this chan-

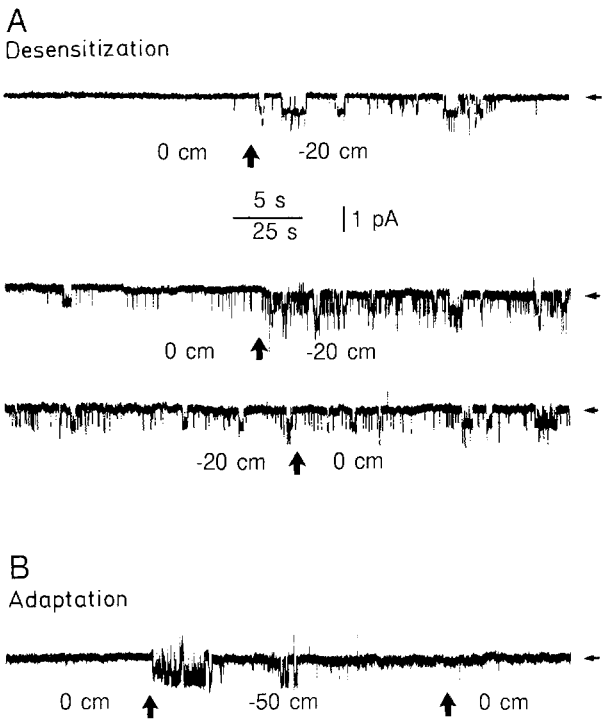

Fig. 4. (*A*) Desensitization of stretch activation in an attached patch. The upper trace shows the first activation of the cation channels with pipette suction. After about 5 min of manipulations with pipette suction (*see* Fig. 3) the activation is repeated successfully in the second trace, but when the suction is relieved in the third trace (second and third traces are continuous), the channels remain activated. (*B*) Adaptation to stretch activation in another patch: upon application of 50 cm H_2O suction to the pipette, the channel is immediately activated but channel activity stops before the suction is relieved. Data obtained at 0-mV bath voltage with NaCl in the electrode.

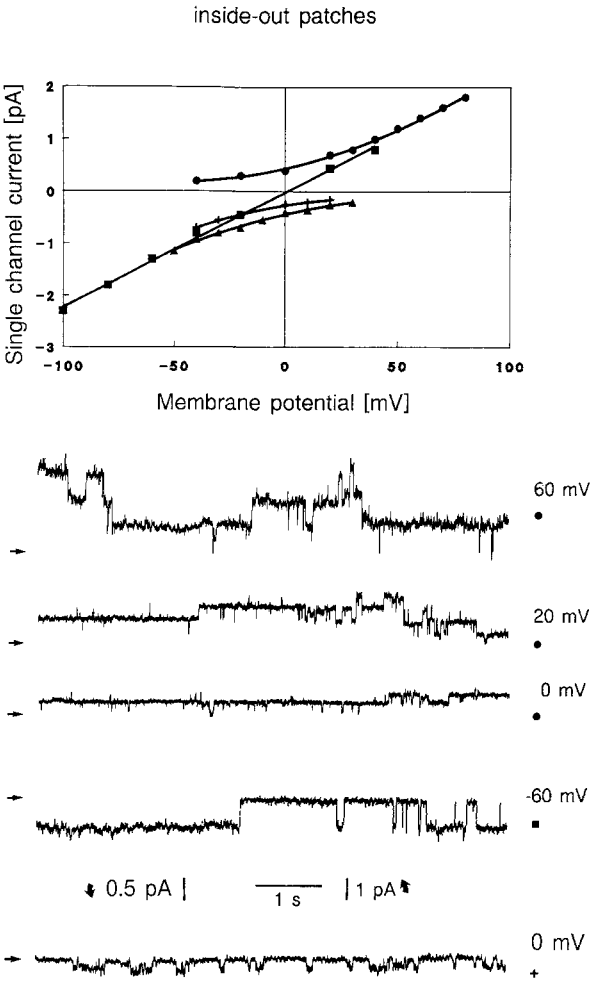

Fig. 5. Data for the SA cation channel in inside-out patches. The upper panel shows the *I-V* curve for four patches with the following solutions (electrode/bath): squares (NaCl/NaCl), triangles (NaCl/NMDGCl), circles (NMDGCl/NaCl), and crosses ($BaCl_2$/NMDGCl). NaCl and NMDGCl are 150 mM; $BaCl_2$ is 100 mM. The lower panel shows recordings of single-channel current at the voltage indicated. The symbol to the right of the current trace corresponds to the symbol on the *I-V* curve.

nel. Gadolinium has recently been shown to block some stretch-activated channels from the outside (Yang & Sachs, 1989). Neither external Gd^{3+} (10, 20 and 10 μM) nor internal Gd^{3+} (10 μM) had any effect on SA channel activity in inside-out patches in the present investigation. It was, however, possible to demonstrate a strong inhibition by 10 μM Gd^{3+} of the RVD response seen after cell swelling (*data not shown*). This is under further investigation.

The Potassium Channel: Inside-Out Patches

Figure 6*A* shows the *I-V* curves for the K channel obtained in inside-out patches. In symmetrical KCl solutions (circles), there is a pronounced curvature of the *I-V* curve with higher conductance for inward currents from pipette to bath (36 pS in the physiological range of −40 to −90 mV) than for outward currents from bath to pipette (15 pS in the range 40–70 mV). When internal K^+ is replaced by Na^+ (squares), only negative single-channel currents from pipette to bath are seen, excluding the possibility of a Cl^- channel. There was no SA cation channels active in these patches. With NaCl on the inside (bath), the slope conductance in the range −50 to −90 mV was 37 ± 6 pS (SEM, n = 6). The channel current traces shown in Fig. 6*B* demonstrate two basically different gating modes. The most commonly occurring mode is the one shown at 50 and −40 mV. At −60 mV is shown a less frequently occurring gating mode where the channel is fully open most of the time. Amplitude histograms show that the single-channel current in this mode is about 20% larger than the current in the normal mode.

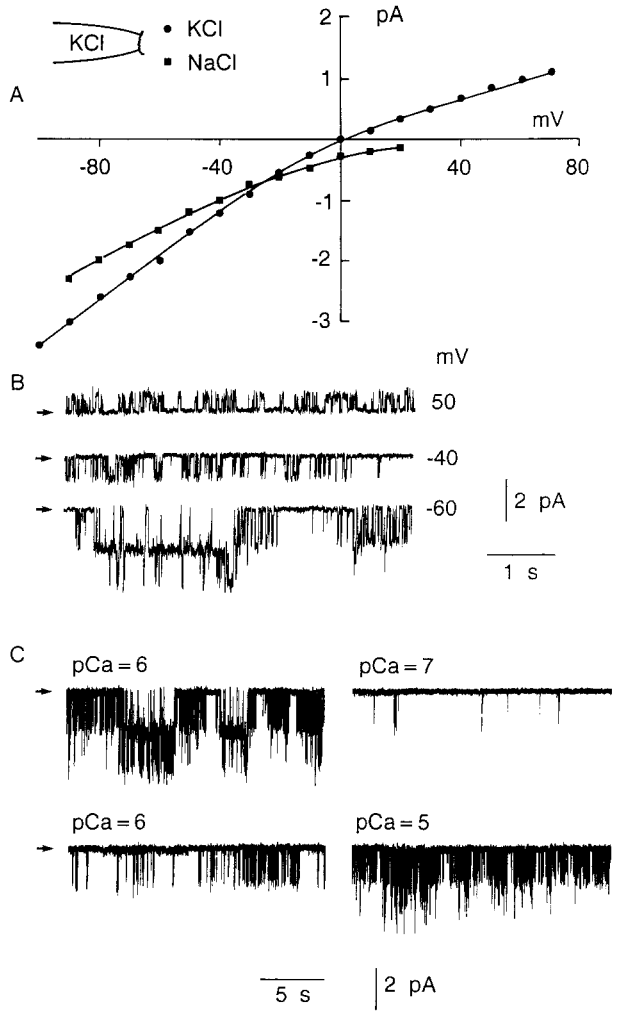

Fig. 6. (*A*) Example of *I-V* curve for the inward-rectifier potassium channel obtained on an inside-out patch with KCl in the electrode and with KCl (●) and NaCl (■) on the inside. In symmetrical 150-mM KCl solutions, the limiting conductance was 36 pS at negative voltages and 15 pS at positive voltages. (*B*) Typical single-channel currents obtained with KCl in the electrode and KCl, pCa = 6 on the inside. Numbers give membrane potential and arrows indicate baseline. Notice two different types of gating at −60 mV. (*C*) Calcium dependence of gating for inside-out patch bathed in KCl on both sides. Membrane potential was −60 mV. The data are sections of a continuous recording and are displayed in chronological order. Notice change in channel activity with time at pCa = 6. The result is typical for three independent experiments.

The inward-rectifier K^+ channel is activated by internal Ca^{2+} ions. An example of this is shown in Fig. 6*C*. At a Ca^{2+} concentration of 0.1 μM there is very little channel activity. The channel is activated at 1 μM Ca^{2+}, and activity is unchanged at concentrations larger than 10 μM. It can be seen that the channel activity was not reproducible at pCa = 6. Such apparently spontaneous variations were commonly seen and indicate that the channel gating is determined by factors other than Ca^{2+}. For example, the gating of the inwardly rectifying K^+ channel in endothelial cells depends on internal ATP. In spite of such variations, internal Ca^{2+} did in all cases activate the channels. We did not observe any significant voltage-dependent gating. The channel could not be activated by suction (negative pressure) and was thus not stretch activated.

The K^+ Channel: Cell-Attached Patches

Most patches showed very little spontaneous K^+ channel activity. Figure 7 gives the *I-V* relationships for the inward-rectifier K^+ channel obtained with KCl and with NMDGCl in the electrode.

The *I-V* curve with K^+ in the electrode is very similar to the one seen in inside-out patches (Fig. 6) in symmetrical solutions of K^+ except for a displacement on the voltage axis created by the cell potential. In 11 patches which showed spontaneous activity, the conductance was 34 ± 4 pS (SEM, n = 8) at negative (hyperpolarizing) bath voltages and 29 ± 3 pS (SEM, n = 11) at positive (depolarizing) bath voltages. This corresponds to the value of 37 ± 6 pS at negative membrane potentials found in isolated patches. The reversal potential (V_{rev}) for the K^+ current was 49 ± 5 mV (SEM, n = 11).

With a value of 187.7 mM for the intracellular K^+ concentration (*see* Table 1) and 150 mM K^+ in the electrode, the K^+ equilibrium potential across the patch (E_K) amounts to −5.7 mV (inside negative). From Eq. (2) the cell membrane potential (V_m) can thus be calculated at 49 − (−5.7) mV = −54.7 mV at room temperature, to be compared with previous measurements at −57 mV, recorded by Gstrein et al. (1987), and −61 mV (Lambert et al., 1989), both measured at 37°C. It is likely that the mere observation of spontaneous K^+ channel activity in a cell-attached patch indicate that the cell membrane potential in the cell under investigation might be hyperpolarized compared to an average cell. This would explain why the membrane potential calculated from K^+ channel recordings is slightly more negative than the membrane potential calculated from the Cl^- channel or the nonselective cation channel (Table 1). The fact that the membrane potentials found in the present investigation are slightly less negative than expected from previous measurements at 37°C is likely to be caused by a lower potassium permeability at 21 than at 37°C.

The Chloride Channel: Cell-Attached Patches

In cell-attached patches, we have found a chloride channel which was first observed in cells swollen

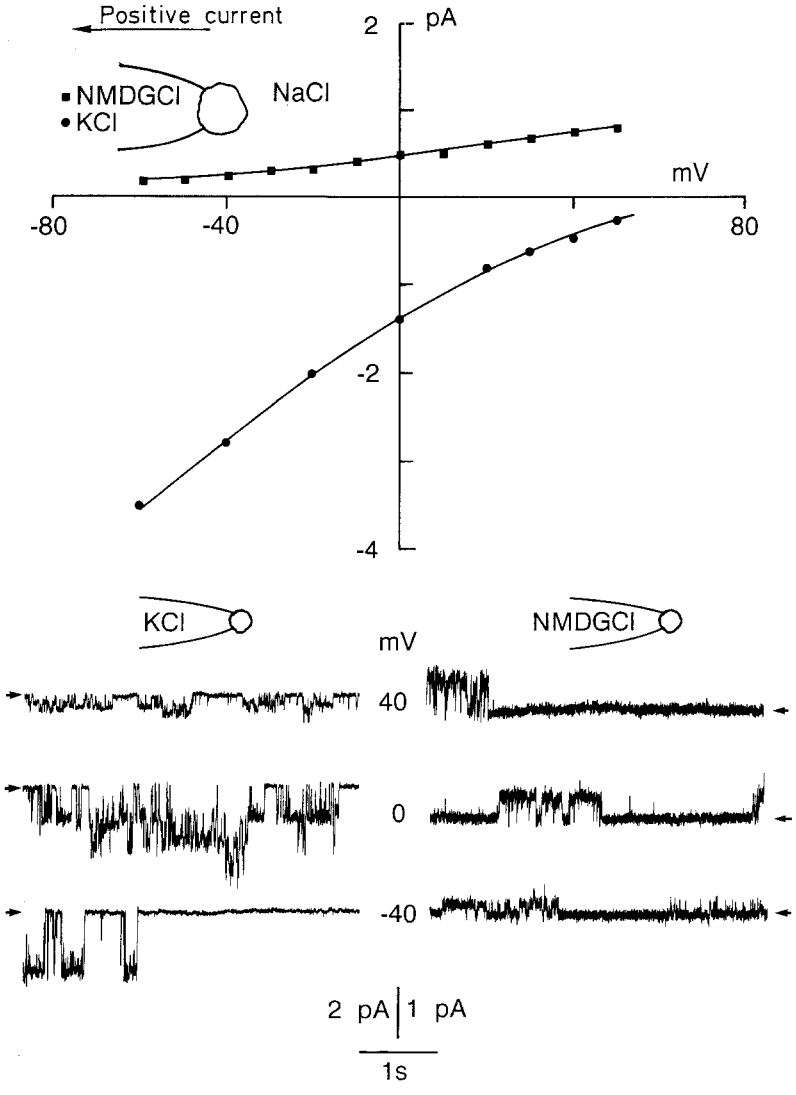

Fig. 7. The upper panel shows the relationship between bath voltage and patch current in cell-attached patches showing spontaneous activity of the inward-rectifier K^+ channel. Data are from a patch with KCl in the pipette (negative current) and with NMDGCl in the pipette (positive current). With external K, the conductance was 37 pS at negative voltages and 22 pS at positive voltages. With external NMDGCl, the conductance at zero bath voltage was 7 pS, increasing at positive voltages to 11 pS. The single-channel K^+ current at zero bath voltage is 0.5 pA at zero external K^+ (NMDGCl) and −1.4 pA at 150 mM external K^+. The lower panel shows typical single-channel currents for the two cases at different potentials. The arrows indicate the baseline.

in hypotonic medium. This channel is rarely seen active in cell-attached patches under isotonic conditions. Since the channel conductance is very low, a detailed description of this channel is difficult. Figure 8 shows some data on the channel.

In cell-attached patches, there seems to be a fully activated and a partly activated form of this channel. Figure 8*A* shows current traces for the fully activated form, corresponding to the *I-V* curve marked with crosses. This is a rare example showing spontaneous activity of the fully activated form. The conductance is 7 pS and the (extrapolated) current reversal voltage is 25 mV. Figure 8*B* shows current traces for a partly activated Cl^- channel with a different gating. These data were obtained after hypotonic stimulation and return to normal tonicity. The conductance was in two experiments 3 and 3.2 pS, respectively, and the current reversal voltage was about 30 mV. The simplest interpretation is that this channel represents a partly activated state of the 7-pS channel. The data presented here were obtained with NMDGCl in the electrode which gives an unambiguous identification of chloride channels in cell-attached patches.

This channel was activated by hypotonic shock in most cell-attached patches (*see below*), and it was also activated when the Ca^{2+} ionophore A23187 was added to the medium bathing the cell. The gating mode in these cases was the fully activated form. The channel was not activated by membrane stretch.

The Chloride Channel: Inside-Out Patches

In inside-out patches with NMDGCl on both sides (bottom panel of Fig. 8), the conductance was 4–5

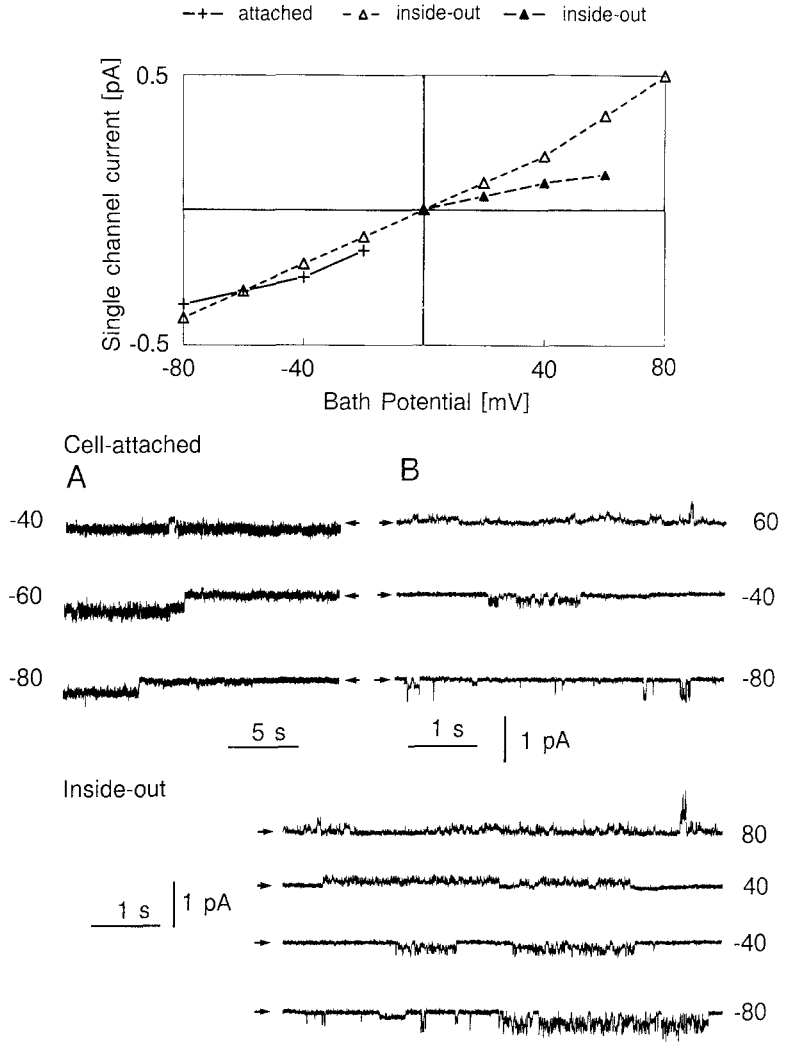

Fig. 8. *I-V* curves and typical current traces for the chloride channel. The values next to current traces are bath voltages (= membrane potential for inside-out patches). (*A*) Current traces for a cell-attached patch corresponding to the *I-V* curve shown with crosses. This is a rare example of spontaneous activity of the fully activated chloride channel. (*B*) Channel activity of the partly activated chloride channel in a cell-attached patch. Notice at 60 and −80 mV the different current levels in the open state. The bottom panel shows current traces of a partly activated channel in an inside-out patch. The open and filled triangles in the *I-V* curve correspond to two types of channels or substates of the same channel. This is best seen in the current tracing at 80 and at −80 mV. The electrode contains NMDGCl for all data. For inside-out patches, the bath was also NMDGCl, and for the cell-attached patches, the cell was bathed in normal tonicity NaCl Ringer's solution.

pS, but there were also levels with a conductance of 1.1 and 2.4 pS in different patches. The open and filled triangles on the *I-V* curve in Fig. 8, upper panel, correspond to two conductance levels and represent either two types of channels or, more likely, substates of the same channel, since they are often observed together. Identical data were obtained with NaCl in the bath (in patches not containing the SA channel). The gating of this channel is indistinguishable from the gating of the partly activated Cl^- channel in cell-attached patches, *cf.* Fig. 8*B* and bottom panel. We have never seen the fully activated form of the Cl^- channel in inside-out patches.

In inside-out patches, channel activity was not dependent on internal Ca^{2+}. The channel could not be activated by suction (negative pressure).

Other Channel Types in Inside-Out Patches

The Large Cl^- Channel

This channel has a conductance around 400 pS when measured with 150 mM Cl^- on both sides (*see* Fig. 9). Similar channels have been reported for many cell types (Blatz & Magleby, 1983, Kolb & Ubl, 1987; Bosma, 1989). One or more of this type of channel was always present in inside-out patches obtained with large electrodes (2 MΩ). This made study of the K^+ channel difficult. In order to avoid the large Cl^- channel, smaller electrodes (6 MΩ) were used. Channel activity for the large Cl^- channel does not depend on internal Ca^{2+}. Open-state probability is zero when membrane potential becomes more negative than −30 to −40 mV. At positive membrane potentials the open-

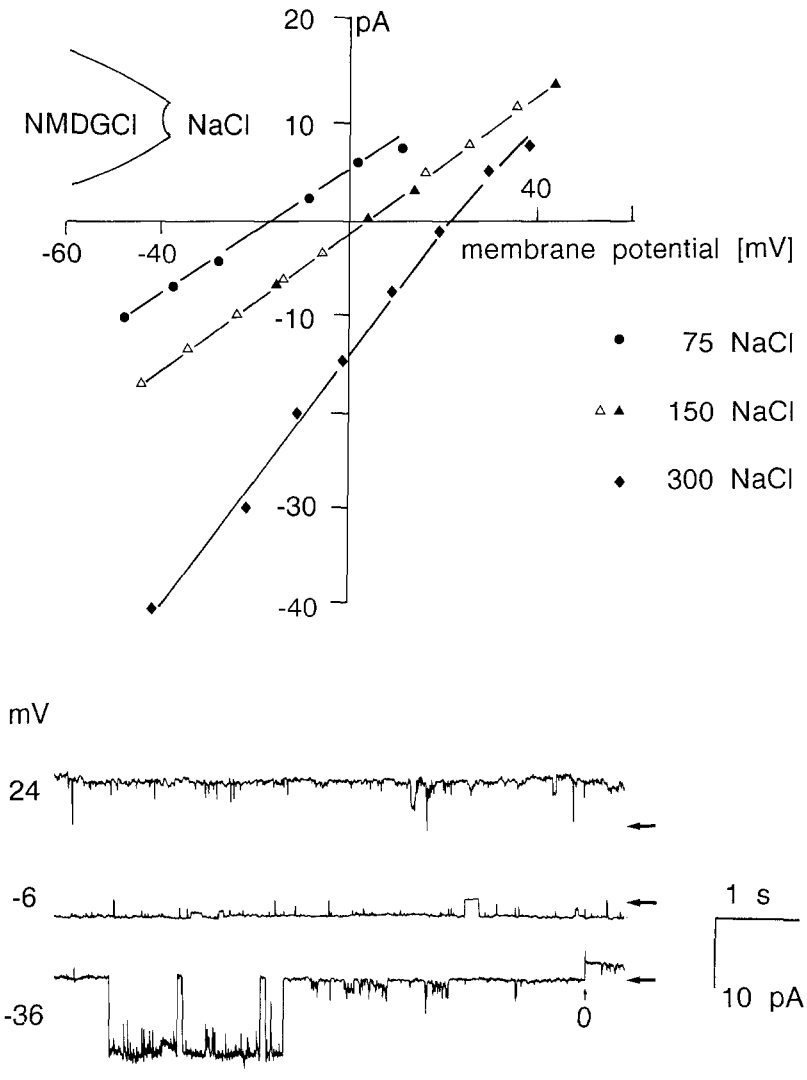

Fig. 9. The large Cl^- channel in an inside-out patch with 150 mM Cl^- on both sides (△▲, indicate separate experiments), 75 mM NaCl on the inside (●) or 300 mM NaCl on the inside (♦). The upper panel shows *I-V* curves. The lower panel gives typical current traces. The values next to the current traces are bath voltages (membrane potentials).

state probability is close to one (*see* Fig. 9, lower panel). The channel is thus activated by voltage. We have never observed this channel in cell-attached patches.

The 34-pS Cl^- Channel

We have also in four inside-out patches from Ehrlich cells seen the chloride channel which was described by Welsh (1986) and by Frizell, Rechkemmer and Shoemaker (1986) for human airway epithelium (Fig. 10). The four patches represent patches with this channel but without the large Cl^- channel, which made impossible observation of other channels simultaneously present in the patch. The channel might therefore be present in higher density than indicated by the four patches. This channel has higher conductance at positive membrane potentials (55 pS) than at negative potentials (≈17 pS). The conductance at 0 mV was ≈34 pS. This channel is proposed to be the conductive pathway which is activated by cAMP (Li et al., 1989). Hudson and Schultz (1988) first observed this channel in inside-out patches of Ehrlich ascites tumor cells, and they claim that the channel was activated during cell swelling produced by uptake of alanine. However from their current recordings, they appear to have observed activation of the SA channel or, in some cases, of K^+ channels. Both types of channels are much more frequently observed in inside-out patches than the 34-pS Cl^- channel. We have never seen this channel in cell-attached patches.

Effect of the Ca^{2+} Ionophore A23187 on Channel Activity in Cell-Attached Patches

In order to study the direct or indirect effect of internal Ca^{2+} on the ion channels in the intact cell

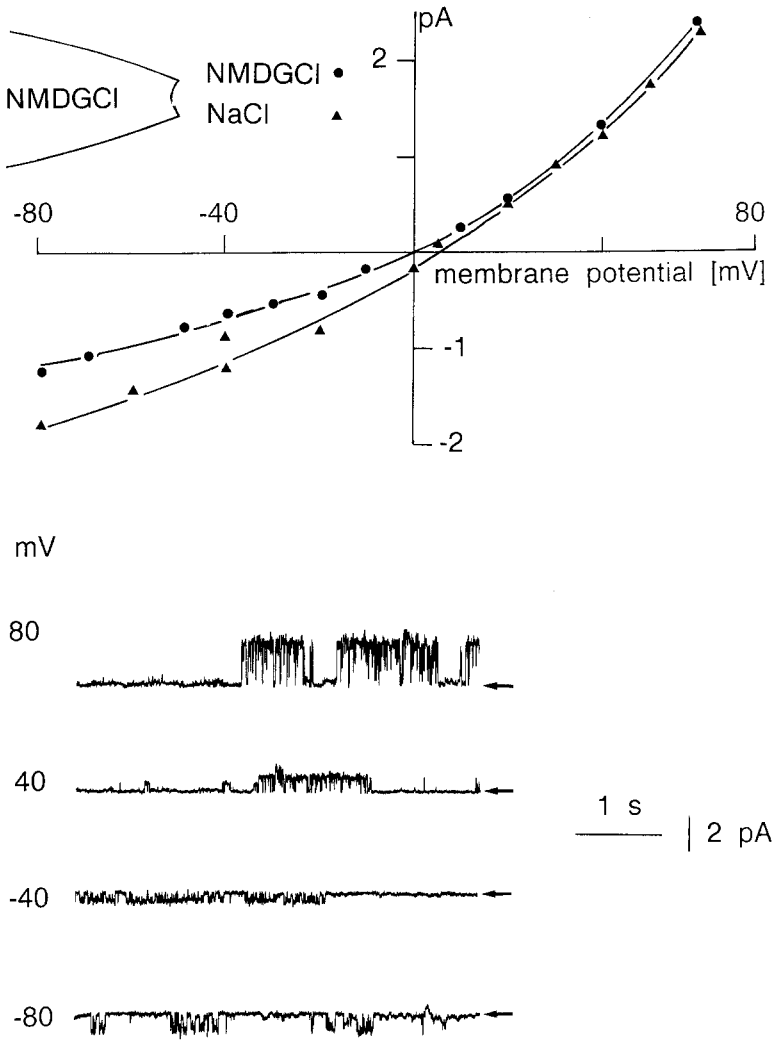

Fig. 10. Inside-out patches showing the 34-pS Cl^- channel. The upper panel shows *I-V* curves with 100 mM NMDGCl on both sides (●) or with 150 mM NaCl in the bath (on the inside) (▲). The lower panel gives typical current traces with NaCl on the inside. Bath voltages (= membrane potential) are indicated.

membrane, we have performed experiments in which 2 μM of the Ca^{2+} ionophore A23187 was added to the medium bathing the cell while the patch current was monitored in cell-attached patches (Fig. 11).

We have separately investigated the effect of A23187 on the inward-rectifier K^+ channel, on the SA cation channel, and on the chloride channel.

The K^+ Channel

The inward-rectifier K^+ channel was activated after addition of A23187 in five of six patches with KCl in the electrode (Fig. 11*A-C*) and in a patch with NaCl in the electrode (Fig. 11*D*). Similar results, as in Fig. 11*D*, are found with NMDGCl in the electrode. Note that with KCl in the electrode (Fig. 11*A-C*) all channel openings lead to negative currents, but with NaCl in the electrode (Fig. 11*D* and *E*) K^+ channel openings will give positive currents and Cl^- channel openings negative currents (*see* Materials and Methods). The activity started 34 ± 6 sec (SEM, $n = 7$) after change to A23187-containing external solution. The change of solution took about 10–20 sec. In most cases the channel activity appeared in bursts of activity of minute-long duration separated by minute-long pauses (Fig. 11*B*). This is taken to indicate that the Ca^{2+} pump becomes activated and removes Ca^{2+} from the cytosol. In Fig. 11*A* only a single burst is seen; Fig. 11*B* shows an example with several bursts. The recording in Fig. 11*C* shows a gradual increase in activity after a time lag of several minutes. Maybe these examples represent situations with different balance between Ca^{2+} entry and Ca^{2+} removal.

The SA Channel

Application of Ca^{2+} ionophore had no apparent effect on the SA cation channel. In 11 patches there

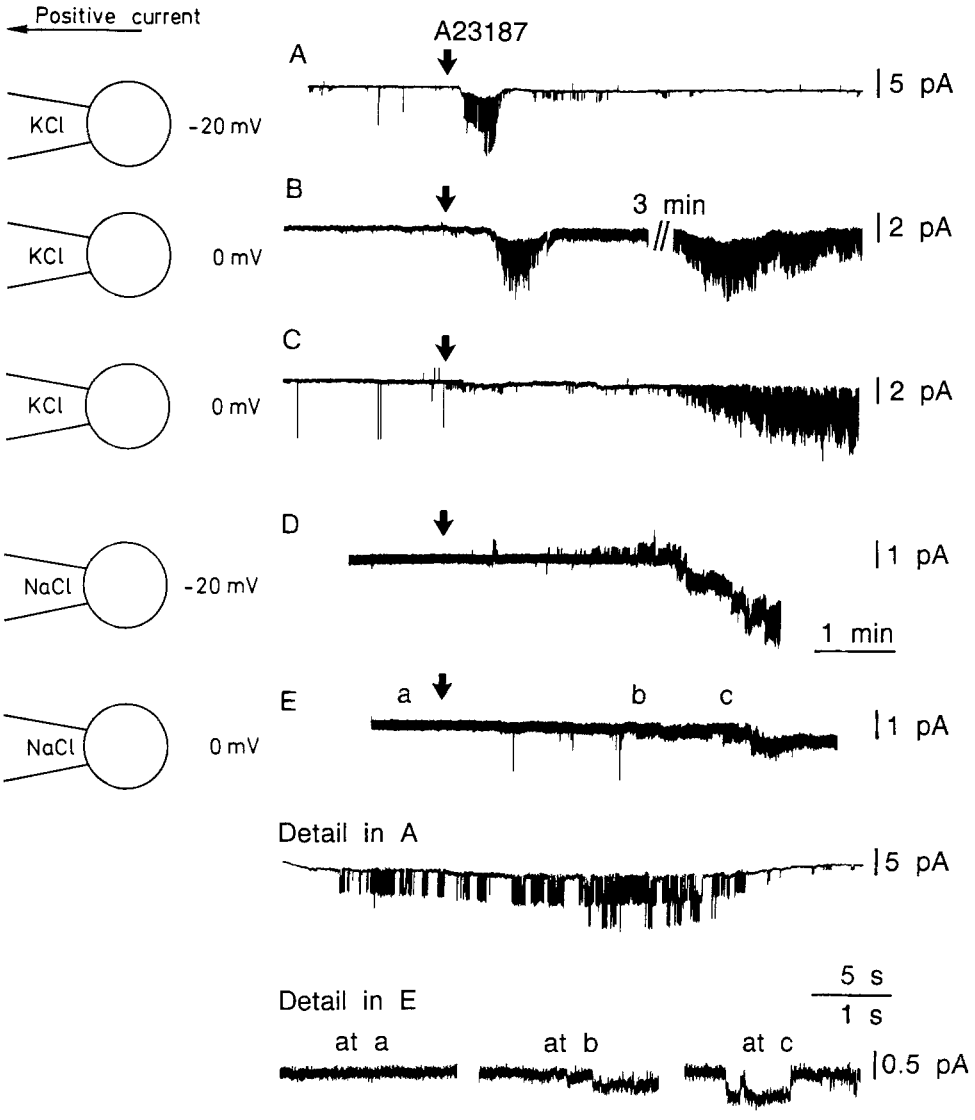

Fig. 11. The patch current in cell-attached patches when 2 μM of the Ca^{2+} ionophore A23187 is added to the bath solution. (*A*, *B* and *C*) Obtained with KCl in the electrode. In these panels, inward K^+ currents are shown as negative (downward) deflections. (*D* and *E*) Obtained with NaCl in the electrode; upwards deflections represent outward K^+ current. In all five panels outward moving chloride (inward current) corresponds to downward deflection. The bath voltage for each panel was (in mV): *A*: −20; *B*: 0; *C*: 0; *D*: −20; and *E*: 0. The vertical arrows indicate the change to Ca^{2+} ionophore-containing medium. The two bottom panels show details on a faster time scale.

was no activity of this channel before application and no activity after application. Five patches showed initial SA channel activity, with low opening probability, $P_o < 0.02$. After change to ionophore-containing medium, there was no systematic change in the open probability. Thus it appears that internal Ca^{2+} has no regulating effect on the SA channel.

This shows that the SA channel is independent of internal Ca^{2+}, but dependent on membrane stretch. Apparently, the channel activity is also independent of possible internal factors mediated by an increase of internal Ca^{2+} and by the hyperpolarization of the cell membrane seen after addition of the Ca^{2+} ionophore (Lambert et al., 1989).

The Chloride Channel

Contrary to this, internal Ca^{2+} seems to influence the activity of the small chloride channel. Figure 11*D* and *E*, show recordings of patch current with NaCl in the electrode. Some minutes after change to 2 μM external A23187, a noisy negative current appears which is due to outward Cl^- movement

(there were no SA channels active in the patch). The patch current from Fig. 11*E* is shown on an expanded scale at the bottom. There is a clear difference between the current before and after stimulation with A23187. The onset of activity of the Cl^- channel shows fairly clear single-channel structure, but when many channels are active (Fig. 11*D*) it is not possible to distinguish single-channel current levels. Apparently the chloride channel has different gating modes. The details from points "*b*" and "*c*" indicate different conductances. Possibly, the detail at "*c*" gives the full current amplitude and the detail "*b*" is a substate with about half conductance. Even when the channel at "*c*" has closed, the baseline is changed, indicating another gating mode.

Simultaneous activation of K^+ and Cl^- channels were often seen. This is most clearly seen in Fig. 11*D* where K^+ currents (upwards deflections) and Cl^- currents (downward deflections) have opposite signs. The baseline deflection occurring simultaneously with the high K^+ channel activity in Fig. 11*A* and *B* is presumably also due to Cl^- activity, which will create a negative current.

The influence of A23187 on the Cl^- channel activity was investigated in 20 patches. Of these, seven were rejected because the baseline was not initially "clean" enough to permit identification of channel activity with this small amplitude. Of the 13 remaining (3 with KCl, 7 with NaCl and 3 with NMDGCl in the electrode), Cl^- channel activity was induced by the Ca^{2+} ionophore A23187 in 10 patches. In three patches, the channel was not stimulated. The average time lag before activation was 67 ± 19 sec (n = 10).

Activation of Channels after Cell Swelling in Hypotonic Solutions

In the cell-attached configuration, an osmotic gradient (extracellular hypotonicity) causes cell swelling followed by a RVD. Therefore, such on-cell mode of the pipette configuration was used to measure the effect of cell swelling on the ion transport systems. The SA cation channel, the inward-rectifier K^+ channel and the Cl^- channel were all activated during volume regulation although to a different degree. The activation of these channels in cell-attached patches during RVD following hypotonic shock to half tonicity are shown in Figs. 13–15. Table 2 gives a schematic presentation of the results.

Change to hypotonic solution was successfully undertaken on 45 patches. The electrode electrolyte were KCl (18 patches), NaCl (19 patches) and NMDGCl (8 patches). In order to determine whether a channel type becomes activated after cell swelling we have, for each type of channel, first selected the patches in which we know that the channel is present, either because it was activated, because it showed spontaneous activity, or because it was observed after the end of the hypotonic stimulation when the patch was isolated as an inside-out patch. Table 2 also gives the change of patch currents due to activation of the three types of channel. The data are scaled to give values corresponding to 0 mV bath voltage, i.e., resting cell potential.

The experimental protocol for the SA channel and the Cl^- channel was in most cases the following: 5-min observation of the reference situation, change to hypotonic solution and 10-min observation, and change to normal tonicity and at least 5-min observation. In our initial protocol for the K^+ channel, we have only 5 to 10 min of observation after hypotonic shock.

The SA Cation Channel

This channel was activated in 13 out of 28 patches in which channel existence was confirmed either by spontaneous channel activity during the preincubation in isotonic medium or by channel activity after formation of an inside-out patch after the end of the experiment. The patches were selected from 18 patches with KCl in the electrode and 19 patches with NaCl in the electrode. Typical activation currents are shown for the SA channel in Fig. 12. Activation in the sense used here means a visually significant change of channel activity. This covers cases with a clear activation (traces *A* and *D*) but also cases like trace *C*, in which the channel is activated but with an extremely low opening probability. Trace *E* shows an extreme case in which there was no activity under hypotonic conditions but where cell shrinkage upon return to normal tonicity activated the channel.

Only very small currents were carried by the SA channel. The open probability of the activated channel in most patches was only 0.02–0.06. Because of this, the time averaged patch current is very low (−0.07 ± 0.04 pA) (*see* Table 2).

For the SA channel there is an almost 20-mV *increase* of reversal potential. This corresponds to an expected 18-mV increase due to dilution of the internal concentration of cations by a factor of 2 (*see below,* "Electrochemical Relations").

The K^+ Channel

Activation of channels was observed in all patches at patch potentials equal to normal cell potential (= zero bath voltage) or at 20- to 40-mV hyperpolariza-

Table 2. Activation of channels following hypotonic shock

Channel type	K^+	SA	Cl^-
Patches known to contain channel	13	28	28
Number of above patches activated	9	13	20
Activation time (sec)	65 ± 10.9(8)	80 ± 7.5(13)	100 ± 14.6(17)
Activated patch current (pA) at V_b = 0 mV	−4 ± 1.1(8)[a]	−0.07 ± 0.04(7)	−0.3 ± 0.09(12)
Reversal potentials			
In all patches (mV)	49 ± 5(11)	34 ± 3(30)	—
In NaCl (mV)	44 ± 6(4)	34 ± 4(7)	—
In ½NaCl (mV)	60 ± 4(4)	54 ± 3(10)	—

[a] With 150 mM K^+ in the electrode.

These data were obtained on 45 cell-attached patches (18 with KCl, 19 with NaCl and 8 with NMDGCl in the electrode). Data for K^+ channel activation were obtained with KCl in the electrode. Data for SA channel activation were obtained with NaCl or KCl in the electrode. Data for Cl^- channel activation were obtained with NMDGCl or NaCl in the electrode. 'Reversal potentials in all patches' is for all patches initially investigated in NaCl before the systematic study of the effects of hypotonic shock was undertaken. 'Reversal potentials in NaCl' and 'in ½NaCl' are in most cases based on paired data before and after stimulation with a few unpaired values. Activated patch current is an estimated mean value over 2–3 min at the maximal activation. It is scaled to 0 mV using the actual value and the reversal potential. For the Cl^- channel currents, a reversal potential of 20 mV was used. The values are given as mean ± SEM with the number of independent experiments in parentheses.

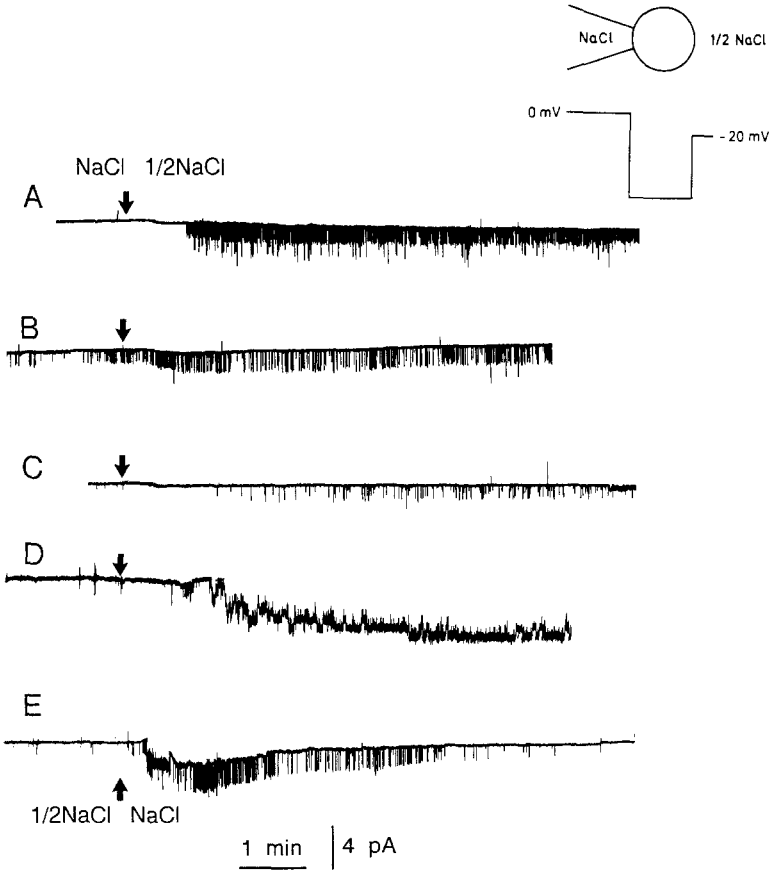

Fig. 12. The influence of hypotonic shock on the activity of the SA channel in cell-attached patches. NaCl in the electrode and −20-mV bath voltage (hyperpolarization of patch). Inward current through the SA channels are shown as negative deflections. The external NaCl Ringers's solution is changed from normal tonicity to half tonicity at the arrow (current traces *A*, *B*, *C* and *D*) or from half tonicity to normal tonicity (trace *E*). Recordings *A*, *B* and *C* show typical reactions to hypotonic shock. Recording *D* shows an extreme case with activation of many SA channels. Recording *E* shows an extreme case of activation following return to normal tonicity.

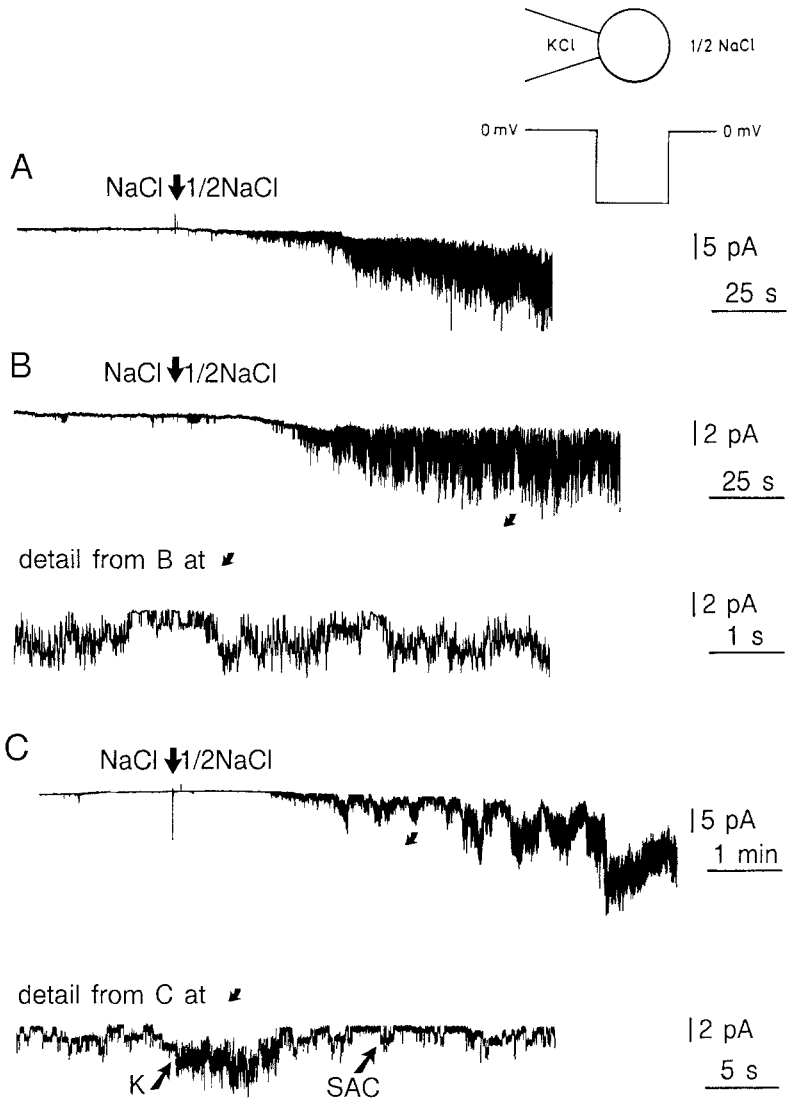

Fig. 13. The activation of K^+ channels in cell-attached patches when the outside medium was changed from normal to half tonicity. The electrode contains KCl and the bath voltage was 0 mV in traces *A* and *B* and −20 mV in trace *C*. Below trace *B* is shown an expanded view of the channel activity. Trace *B* shows induced activity of both the SA channel and of the K^+ channel. The SA channels give a rather steady activity, whereas the K^+ channels give bursts of activity. The K^+ channels have somewhat larger single-channel amplitude than the SA channels. This is illustrated in the detail on an expanded time scale below trace *C*.

tion. Under these circumstances, the K^+ channel can be observed with certainty only if the electrode contains KCl, in which case K^+ channel openings lead to negative currents. The positive K^+ currents from the cell into an electrode containing NaCl or NMDGCl are too small to be reliable when observed in the presence of other active channels (*cf.* Fig. 7). We have observed activation of K^+ channels with NaCl in the electrode (*cf* Fig. 11), but failure of activation could easily mean that the current amplitude is actually too small to allow observation when other channels in the patch are activated. We therefore used mainly patches with KCl in the electrode for swelling experiments. Of 18 patches examined, the existence of the K^+ channel was confirmed in 13 patches and of these K^+channels were activated in 9 patches. Figure 13 shows some examples of K^+ channel activation. The most common picture is the one shown in trace *C*. The characteristic feature is that K^+ activity occurs in waves and that the activity often is so high that it becomes impossible to distinguish clear unitary K^+ currents. In trace *C* we also see activation of the SA channel which is much more steady than the K^+ current and usually with slower kinetics (*see* Fig. 13, lower panel). The time for onset of channel activity after hypotonic shock was 65 ± 31 sec (SD, $n = 8$). The single-channel current reversal voltage (V_{rev}) increases from 49 to 60 mV during cell swelling. This is 7 mV less than the 18-mV (25.3 × ln 2) increase in V_{rev} which could be expected due to a factor 2 dilution of internal K^+ provided the cell membrane potential stayed constant. This indicates that a 7-mV depolarization of the cell membrane is seen after cell swelling at room temperature compared to a 20-mV depolarization after cell swelling at 37°C (Lambert et al., 1989) (*see also below*, "Electrochemical Relations").

The K^+ channels activated gave rise to an in-

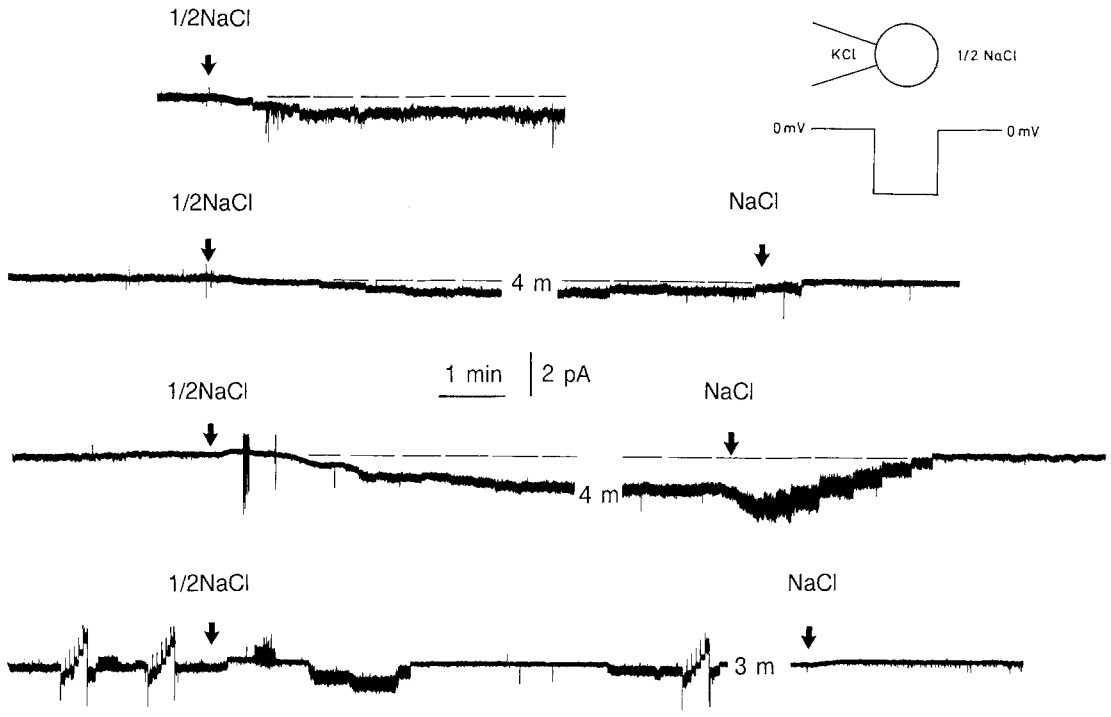

Fig. 14. Activation of the chloride channel by hypotonic shock in four cell-attached patches with KCl in the electrode and 0-mV bath potential. At the first arrow on each trace, the external medium is changed from normal tonicity Ringers to half tonicity and at the second arrow, the medium is returned to normal tonicity. The current trace at the bottom is interrupted by three intervals where voltage was changed to obtain an *I-V* curve. Downward deflections from baseline are due to outward Cl^- movement. Upward deflections at the bottom trace are due to outward K^+ movement. Notice that the baseline level is unchanged after the experiment.

ward current (KCl in electrode) through the patch of typically -4 ± 3 pA (SD, $n = 8$) (*see* Table 2).

The Cl^- Channel

This channel was activated in 20 patches out of 28 in which Cl^- channel existence was confirmed by spontaneous activity in isotonic medium during preincubation or by the channel activity after the hypotonic chock. Most data are from patches with NMDGCl and NaCl in the electrode, in which case Cl^- channel openings lead to negative currents seen as downward deflections (outward movement of Cl^-). Figure 14 shows activation of the Cl^- channel in four current traces. The single-channel currents are so small that the unitary nature of the patch current is easily overlooked. The channels seem to activate in an all or none fashion rather than gradually to change the open probability. In the third trace, the changes in current during the first minutes do not appear to have much single-channel nature.

Upon return to normal tonicity of the external medium, the current first increases and then decreases in a stepwise fashion as the individual Cl^- channels inactivate. The initial increase in current is due to the increase of internal chloride concentration after the cell shrinkage. Closure of the channel after returning to isotonic medium is also seen in the second trace. The upper and bottom traces show very clearly the unitary nature of the current. Although the contribution to the current (chloride outflux) from the single channels is very small, the contribution to the electrical current across the patch is much larger than the contribution from the SA channels (*see* Table 2). After 5 to 10 min of RVD, Cl^- channels were active in most patches. This activity disappeared however within 0.5 to 2.5 min after return to normal external tonicity. Thus, the small Cl^- channel is dramatically activated during RVD in hypotonic medium and closed when the medium again is made isotonic.

Electrochemical Relations

In Table 1, we have evaluated the expected current reversal voltages (V_{rev} *see* Eq. (2)) for the K^+ channel, the Cl^- channel, and the SA cation channel both for normal cells (reference situation) and for hypotonically swollen cells. A cell membrane potential (V_m) is either -57 mV (Gstrein et al., 1987) or -61 mV (Lambert et al., 1989) for cells in isotonic

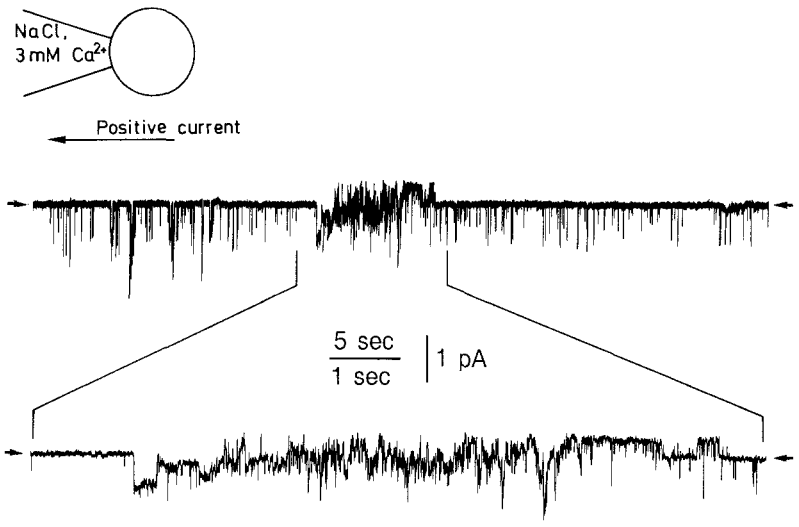

Fig. 15. Current trace from an attached patch with spontaneous activation, first of the SA channel and then of the K^+ channel. Note that Na^+ influx via the SA cation channel is seen as downward current deflections and K^+ efflux via K^+ channels as upward current deflections. Lower trace is an expansion of upper trace. The electrode contained NaCl with 3 mM $CaCl_2$ added. Bath voltage was 0 mV. The figure represents three independent experiments.

reference situation and −41 mV for cells in hypotonic solution (Lambert et al., 1989). The ionic equilibrium potentials are calculated from previous estimations of the cellular ionic concentrations (*see* legend to Table 1).

After the initial swelling following hypotonic shock, the intracellular concentrations attain one-half of their initial value. This produces a 25.3 × ln 2 mV = 17.5-mV shift of equilibrium potential. Provided the cell membrane is depolarized after cell swelling, the shift of reversal potential will be smaller. It can be seen from Table 1 that only a minor depolarization seems to take place. The estimated depolarization is only 7 and 0 mV from measurements on the K^+ channel and the nonspecific cation channel, respectively, both measured at 21°C. At 38°C a depolarization of 20 mV at 150 mOsm (Lambert et al., 1989) and 10 mV at 225 mOsm (Gstrein et al., 1987) has been reported.

Concurrent Activation of Nonselective, Stretch-Activated Cation Channels and Ca^{2+}-Activated K^+ Channels

In experiments with Ca^{2+}-containing NaCl solutions (3 mM Ca^{2+}) in the pipette, concurrent activation of SA cation channels and K^+ channels was consistently observed (*see* Fig. 15). Spontaneous activation of a SA cation channel, seen as downward current deflection, is followed after about 20 sec by activation of a K^+ channel (upward current deflection) taken to represent the inward-rectifier K^+ channel.

We interpret this as follows: the initial activation of the SA channel leads to influx of Ca^{2+} from the electrode into the cell. This again results in activation of neighboring K^+ channels in the patch. In a series of previous experiments with activation of SA channels by electrode suction and with no Ca^{2+} in the NaCl electrode solution in the pipette, a similar delayed K^+ channel activation was very seldom observed. A more systematic investigation of this coupling between the SA cation channel and the inward-rectifier K^+ channel has not yet been undertaken.

Discussion

Nonselective Cation Channels Activated by Stretch

The conductance to Na^+ was measured at 24 pS in cell-attached patches as well as in inside-out patches, indicating that the same channel is indeed present in inside-out and in cell-attached patches. Also, the channels can be stretch activated by electrode suction in both types of patches, which furthermore substantiates this identity. The channel is, however, usually closed in cell-attached patches, unless deliberately provoked to be active, and it is usually open in excised patches. In some cell-attached patches the channel fluctuates (*see* Fig. 2*D*). The complexity of regulation of these channels may indicate that they are modulated by more than direct membrane stretch.

Guharay and Sachs (1984) have advanced the idea that the SA channels are attached to the cytoskeletal strands and that channels open when membrane stretch is transmitted to the channel through this network. Thus, the cytoskeleton has been proposed (Sachs, 1986, 1987, 1988) as the sensor and mechano-transducer of SA channel activa-

tion. It is tempting to suggest the desensitization and adaptation phenomena described in the present paper as being due to mechanical relaxation in the cytoskeleton network following deformation.

SA cation channels conducting both mono- and divalent cations (e.g., Na^+, K^+, and Ca^{2+}) have been observed in a variety of biological systems: in endothelial cells (Lansman et al., 1987), frog oocytes (Taglietti & Toselli, 1988), smooth muscle (Kirber et al., 1988), ascidian oocytes (Moody & Bosma, 1989), in an osteoblast-like cell line (Duncan & Misler, 1989), in the stretch receptor organ of the crayfish (Erxleben, 1989), in *Xenopus* oocytes (Yang & Sachs, 1989), neuroblastoma cells (Falke & Misler, 1989), and in a variety of epithelia, including: choroid plexus (Christensen, 1987), intestine (Okada, Hazama & Yuan, 1990), opossum kidney cells (Ubl, Murer & Kolb, 1988), juxtaglomerular cells (Kurtz, 1990), and medullary thick ascending limb cells (Taniguchi & Guggino, 1989). For a recent comprehensive review on mechano-sensitive channels *see* (Morris 1990).

The Ca^{2+} Activated K^+ Channel

The results presented above indicate that the surface membrane of Ehrlich cells contains inwardly rectifying calcium-dependent potassium channels. The channel conductance for inward currents was estimated at 40 pS and the conductance for outward currents at 15 pS. Single-channel openings could be triggered in inside-out patches at internal Ca^{2+} concentrations 1 μM or higher. In the second part of this work, it is shown, using cell-attached patches, that the same K^+ channel is activated by cell swelling and by addition of Ca^{2+} plus ionophore A23187.

Potassium-selective channels with similar conductance and *I-V* characteristics have previously been characterized in other cellular preparations like: human erythrocytes (Grygorczyk & Schwartz, 1983), HeLa cells (Sauvé et al., 1986), aortic endothelial cells (Sauvé et al., 1988), renal epithelial cells (MDCK) (Friedrich et al., 1988), and rabbit proximal tubule cells (Parent, Cardinal & Sauvé, 1988). All these channels have a similar Ca^{2+} dependence on the channel activation with little or no influence of membrane potential on open probability. Sauvé et al. (1988) also report the two different kinetic forms we have found in the present channel.

Previous measurements of the K^+ conductance in standard salt solution after Ca^{2+} activation have indicated a cellular K^+ conductance of 134 μS/cm^2 (Lambert et al., 1989). The channel conductance at 5 mM external K^+ (standard salt solution) may be estimated from Fig. 7 (the curve representing NMDG in the electrode) to about 7 pS. From these data we estimate the number of Ca^{2+}-activated K^+ channels in the Ehrlich cell at $\sim 20 \times 10^6$ cm^{-2} or about 250 per cell (using a surface area of 1381 μm^2/cell (Hoffmann et al., 1986)). This estimate assumes an open-state probability (P_o) of 1 for the Ca^{2+}-activated K^+ channel, which is rather unlikely. Thus, the estimate of channel density can be regarded as a minimum. It is tempting to suggest that the volume-induced conductive K^+ transport seen in many cells is always mediated by this type of Ca^{2+} activated channels; this may, however, be an oversimplification (*see* Hoffmann & Ussing, 1992).

The Small Chloride Channel

We propose the hypothesis that the small Cl^- channel activated by cell swelling and by Ca^{2+} ionophore in cell-attached patches, the spontaneous active small Cl^- channel occasionally seen in cell-attached patches and the small Cl^- channel seen in isolated patches are all identical.

The similarity between the channel in isolated patches and the "partly activated" channel in cell-attached patches is strongly indicated by the identical channel gating behavior shown in Fig. 8*B* and bottom panel. The conductance with 150 mM NMDGCl on both sides was 5 pS and the conductance in cell-attached patches with about 65 mM cellular Cl^- (*see* Table 1) was 3 pS which is quite reasonable because most of the *I-V* curves for the channel correspond to outward movement of Cl^-, where the conductance tends to reflect internal Cl^- concentration.

The similarity between the fully and partly activated channel in cell-attached patches was assumed in order not to introduce more channels than necessary. We have only one conductance value for the fully activated channel (7 pS) which is rather different from the value of 3 pS for patches with "partly activated" channels. However, there is not significant basis to postulate two small Cl^- channels due to the difference in conductance. Also, if the "partly activated" channel is a pre-stage to the fully activated channel, it seems not unreasonable that the fully activated channel should have the largest conductance.

For the "partly activated" channel, there seems to be many different conductance levels. We do not presently know whether these levels represent other Cl^- channels or substates of the larger channel. The kinetics of the smaller levels often show a more 'box-like' character while the kinetics of the larger level is more burst-like, with many excursions to a state of about half conductance (Fig. 8, bottom panel at

−80 mV). It is tempting to suggest that the larger channel is a polymer of several smaller units some of which are seen as individual levels.

The channel is fully activated in cell-attached patches either by cell swelling or by addition of the Ca^{2+} ionophore A23187. In inside-out patches, internal Ca^{2+} had no effect on channel gating. This indicates that activation by Ca^{2+} ionophore is an indirect consequence of a cascade of events initiated by an increase in internal Ca^{2+} and leading to activation of the small Cl^- channel (*see below*). We have never been able to activate the 400-pS Cl^- channel or the 34-pS Cl^- channel by neither A23187 or by hypotonic shock.

Comparison with Other Cl^- Channels

Christensen et al. (1989) have reported a Cl^- channel in the choroid plexus epithelium from *Necturus* with a conductance of 7 pS with 112 mM Cl^- on both sides. The channel was activated during volume regulation after hypotonic shock and had a conductance of 2 pS in cell-attached patches. Also, the channel gating seems rather similar to the present channel in the fully activated mode.

F. Pedersen and O. Christensen (*unpublished data*) have observed a Cl^- channel in human sweat duct epithelial cells. Both conductance and gating in inside-out patches were similar to the data observed here for the partly activated Cl^- channel.

Marty, Tan and Trautmann (1984) have reported Cl^- channels of estimated 2–5 pS unitary conductance in rat lacrimal glands. The channels were activated by external carbamylcholine and by external Ca^{2+} ionophore. In contrast to the present channels, they seem to be activated directly by internal Ca^{2+} in inside-out patches.

Swelling Activation

When Ehrlich cells are suspended in hypotonic medium, a RVD response occurs which decreases the Na^+ permeability, but greatly increases both the K^+ and Cl^- permeability and causes a net efflux of K^+ and Cl^- with a concomitant loss of cell water, to restore cell volume (*see* e.g., Hoffmann & Simonsen, 1989). The K^+ and Cl^- channels activated by cell swelling as characterized in patch-clamp studies are described above.

If the K^+ and the Cl^- channel are to account for the export of K^+ and Cl^- during the phase of RVD, then there must be an approximate identity between the K^+ current and the Cl^- current. The K^+ current from pipette to cell is measured at −4 pA with 150 mM K^+ in the electrode at zero bath voltage (*see* Table 2). For a low K^+ medium (standard Ringer solution) in the pipette this would correspond to about 1 pA of outward current through the K^+ channel(s) in the patch. This can be estimated from data for K^+ current amplitude at zero bath voltage with KCl and NMDG in the electrode, respectively (*see* Fig. 7) as $-4\ (^{0.5}/_{-1.4})$ pA ~ 1 pA. The corresponding Cl^- current through the patch is −0.3 pA (*see* Table 2). It is likely that the remaining negative current represents efflux of HCO_3^-, since we have demonstrated an acidification during RVD (*see* Hoffmann & Kolb, 1991).

From the measured single-channel conductance at 7 pS (Fig. 7, *see above*) and 7 pS (Fig. 8, *see above*) for the K^+ and Cl^- channels, respectively, and the K^+ and Cl^- conductances after cell swelling at 19 and 41 $\mu S/cm^2$, respectively (Lambert et al., 1989), the number of volume-activated K^+ and Cl^- channels in the Ehrlich cell can be estimated at 3×10^6 and 6×10^6 cm^{-2} assuming $P_o = 1$. This corresponds to about 40 "swelling-activated K^+ channels" and 80 "swelling-activated Cl^- channels" per cell, or only 0.3 active K^+ channel and 0.6 active Cl^- channel per mean patch area (approx. 10^{-7} cm^2).

In Ehrlich cells it has been shown that the stimulation of channel activity during RVD is "triggered" by an average increase in cell volume that does not exceed 5% (Hudson & Schultz, 1988). The actual mechanism of activation of the RVD response is, however, still only partly understood, and several factors have been assigned a regulatory function, e.g., Ca^{2+}, calmodulin, cAMP, eicosanoids, polyphosphoinositide metabolism, protein kinases, and the microfilament network. Factors which have been proposed to play a role in the RVD response in Ehrlich cells are shown in Fig. 16 of Hoffmann et al. (1988).

There is evidence that Ca^{2+} and calmodulin play a role in RVD in Ehrlich cells: the response is reduced in Ca^{2+}-depleted cells, is accelerated by a stepwise increase in external Ca^{2+} or by addition of the Ca^{2+} ionophore A23187 during the volume recovery, and is inhibited by anti-calmodulin drugs. Moreover, addition of ionophore A23187 in isotonic medium induces a KCl loss which shows several parallels to the volume-induced KCl loss seen during RVD. The KCl loss induced by cell swelling and by addition of ionophore A23187 are, however, also occurring in Ca^{2+}-free media containing excess EGTA, showing that Ca^{2+} entry across the cell membrane is not a necessity and suggesting a role for Ca^{2+} release from internal stores (*see* Hoffmann, Simonsen & Lambert, 1984; Hoffmann et al., 1986).

Based on tracer flux measurements and measurements of the membrane potential using a fluo-

rescent probe and employing an improved calibration technique we have demonstrated a substantial Ca^{2+}-induced increase in conductive P_K and P_{Cl} (Lambert et al., 1989). In the present experiments we find that the same inward-rectifier K^+ channel is activated in Ehrlich cells after cell swelling and after addition of the Ca^{2+} ionophore A23187. The activation of the K^+ channel in inside-out patches bathed in KCl on both sides and at a membrane potential at -40 mV takes place after an increase in $[Ca^{2+}]_i$ from 10^{-7} to 10^{-6} M, which is in the physiological range, supporting the hypothesis that the volume-induced K^+ transport is mediated by the Ca^{2+}-activated K^+ channels.

The Cl^- channel cannot be activated by Ca^{2+} in inside-out patches. The activation of Cl^- channels in intact Ehrlich cells by increase in intracellular Ca^{2+} is probably an indirect effect caused by a stimulated synthesis of leukotrienes. For a recent review of the role of Ca^{2+} in cell volume regulation, *see* Pierce and Politis (1990).

The nature of the sensory mechanisms detecting the volume changes during RVD is, as yet, totally unknown. We have in the present investigation demonstrated nonselective cation channels which can be activated either by cell swelling or by mechanical stress (suction).

The volume activation of the SA channels is variable (*see* Fig. 13). Often we observed that, where it was impossible to activate the channel by suction, it was activated by cell swelling. After prolonged hypotonic cell swelling, channel activation could also be observed following restoration of tonicity (*see* Fig. 12, trace *E*). It is presumably so, that the channel is activated during deformation of the cell which sets up a tension in the cytoskeletal strands connected to the channel. We have previously demonstrated that cytochalasin B which disrupts the actin filaments inhibits the RVD (*see* Hoffmann & Kolb, 1991). It is interesting to note that the activation of the SA channels after cell swelling does not occur instantaneously but seems to be correlated to a certain cell size, which is usually reached after 0.5–1 min. At that time the cell will be at least 25% swollen. Disregarding membrane infoldings, Sackin (1989) estimated for a spherical cell that membrane stretch induced by cell volume increase as small as 1% will be sufficient for SA channel activation. Cells are, however, not osmometric balloons. They can expand membrane folds when subjected to hypotonic swelling. Volume-activated channels have previously been demonstrated in Ehrlich cells after a volume increase of only 5%. The 0.5–1 min delay in SA channel activation (*see above*) may perhaps reflect the involvement of other factors rather than simply the degree of swelling. It is possible, for example, that the acidification occurring during RVD (*see* Hoffmann & Kolb, 1991) can affect the attachment of the actin filaments to the membrane proteins.

The SA channel described here is a nonselective cation channel. This property seems to contradict an involvement of SA channels as pathways for the K^+ and Cl^- efflux. The volume-activated K^+ and Cl^- channels described above *cannot* be activated by mechanical stress (suction). Therefore, it seems likely that the function of these stretch-activated channels is correlated with their Ca^{2+} permeability. A resulting increase in $[Ca^{2+}]_i$ could be part of the volume-activated signal system.

The fact that Ba^{2+} (and hence presumably Ca^{2+}) passes through the SA channel means that a change in volume gives rise to Ca^{2+} influx into the cell. The rise in internal calcium activates K^+ channels directly and Cl^- channels via some intermediate Ca^{2+}-dependent step. These channels mediate a net outflux of K^+ and Cl^- which through the osmotic drag leads to a decrease of cell volume. The SA channel would thus be part of the triggering mechanism for initiating the RVD, as suggested by Christensen (1987) for amphibian choroid plexus cells.

The activity of the K^+ channel induced by swelling often occurred in 'waves' (*see* Fig. 12) which was not the case for the Cl^- channel. If the waves of K^+ activity represent oscillations of internal Ca^{2+} then the conclusion from the more steady Cl^- activity is again that the activity is initiated by a rise of internal Ca^{2+} but does not reflect the actual immediate Ca^{2+} level. This is consistent with the K^+ channel being directly dependent on internal Ca^{2+} (Fig. 6), whereas the Cl^- channel seems to have an indirect dependence because it is not activated by internal Ca^{2+} in inside-out patches.

There seems to be a quantitative mismatch between the amount of Ca^{2+} that would enter the cells and the amount necessary to turn on Ca^{2+}-sensitive K^+ channels. At physiological Ca^{2+} concentration the Ca^{2+} current is very small through the SA channels. The estimated cation current is 1400 fA per channel, thus there will be only about 20 fA of Ca^{2+} current through the open channel. For channels further than 1 μm apart, the diffusion equations predict that 0.5 μm from the channel the excess Ca^{2+} will be less than 8 nM. In order to activate any Ca^{2+}-activated K^+ channels, the K^+ channels would have to be extremely close to the SA channels to provide direct coupling or else both channels would have to be in a confined space that would allow the Ca^{2+} to build up to reasonable level, e.g., between the endoplasmic reticulum and the plasmalemma. Alternatively, some second messenger (e.g., IP_3) could be developed in a confined space and amplify the

signal by releasing stored Ca^{2+}. The finding of concurrent activation of SA channels and K^+ channels in the presence of 3 mM Ca^{2+} in the electrode (*see* Fig. 14) might support the notion of a close spatial relation between SA and K^+ channels.

Although the hypothesis that Ca^{2+} entry via SA channels could be part of the volume-activated signal system is attractive, it has to be remembered that many cells including Ehrlich cells can show a RVD response also in the absence of external Ca^{2+}, suggesting a causal role for volume-induced Ca^{2+} mobilization from internal stores. In addition, it should be recalled that a significant cell depolarization during RVD has been observed for several cell systems including Ehrlich cells (*see* Hoffmann & Ussing, 1992) and may play a role in K^+ channel activation; such depolarization will be enhanced by the activation of nonselective, stretch-activated cation channels. A more complete understanding of the contribution of the SA channel to RVD in Ehrlich cells would require, among other approaches, monitoring of "whole-cell" membrane potential and currents during volume regulation in the presence and absence of specific inhibitors of the SA channels.

References

Blatz, A.L., Magleby, K.L. 1983. Single voltage-dependent chloride-selective channels of large conductance in cultured rat muscle. *Biophys. J.* **43**:237–241

Bosma, M.M. 1989. Anion channels with multiple conductance levels in a mouse B lymphocyte cell line. *J. Physiol.* **410**:67–90

Chamberlin, M.E., Strange, K. 1989. Anisosmotic cell volume regulation: A comparative view. *Am. J. Physiol.* **257**: C159–C173

Christensen, O. 1987. Mediation of cell volume regulation by Ca^{2+} influx through stretch-activated channels. *Nature* **330**:66–68

Christensen, O., Simon, M., Randlev, T. 1989. Anion channels in a leaky epithelium. A patch clamp study of choroid plexus. *Pfluegers Arch.* **415**:37–46

Christensen, O., Zeuthen, T. 1987. Maxi K^+ channels in leaky epithelia are regulated by intracellular Ca^{2+}, pH and membrane potential. *Pfluegers Arch.* **408**:249–259

Duncan, R., Misler, S. 1989. Voltage-activated and stretch-activated Ba^{2+} conducting channels in an osteoblast-like cell line (UMR 106). *FEBS Lett.* **251**:27–31

Erxleben, C. 1989. Stretch-activated current through single ion channels in the abdominal stretch receptor organ of the crayfish. *J. Gen. Physiol.* **94**:1071–1083

Falke, L.C., Misler, S. 1989. Activity of ion channels during volume regulation by clonal N1E115 neuroblastoma cells. *Proc. Natl. Acad. Sci. USA* **86**:3919–3923

Friedrich, F., Paulmichl, M., Kolb, H.-A., Lang, F. 1988. Inward rectifier K channels in renal epitheloid cells (MDCK) activated by serotonin. *J. Membrane Biol.* **106**:149–155

Frizzell, R. A., Rechkemmer, G., Shoemaker, R.L. 1986. Altered regulation of airway epithelial cell chloride channels in cystic fibrosis. *Science* **233**:558–560

Grygorczyk, R., Schwartz, W. 1983. Properties of the Ca^{2+}-activated K^+ conductance of human red cells as revealed by the patch-clamp technique. *Cell Calcium* **4**:499–510

Grygorczyk, R., Schwarz, W., Passow, H. 1984. Ca^{2+}-activated K^+ channels in human red cells. Comparison of single-channel currents with ion fluxes. *Biophys. J.* **45**:693–698

Gstrein, E., Paulmichl, M., Lang, F. 1987. Electrical properties of Ehrlich ascites tumor cells. *Pfluegers Arch.* **408**:432–437

Guharay, F., Sachs, F. 1984. Stretch-activated single ion channel currents in tissue-cultured embryonic chick skeletal muscle. *J. Physiol.* **352**:685–701

Hamill, P., Marty, A., Neher, E., Sakman, B., Sigworth, F.J. 1981. Improved patch-clamp techniques for high-resolution current recoding from cells and cell-free membrane patches. *Pfluegers Arch.* **391**:85–100

Hoffmann, E.K. 1978. Regulation of cell volume by selective changes in the leak permeabilities of Ehrlich ascites tumor cells. *In:* Alfred Benzon Symposium XI. Osmotic and Volume Regulation. C.B. Jørgensen and E. Skadhauge, editors. pp. 397–417. Munksgaard, Copenhagen

Hoffmann, E.K., Kolb, A. 1991. The mechanisms of activation of regulatory volume responses after cell swelling. *In:* Volume and Osmolarity Control in Animal Cells. R. Gilles, L. Bolis, and E.K. Hoffmann, editors. ACEP Series, Vol. 9, pp. 140–177. Springer-Verlag, Heidelberg

Hoffmann, E.K., Lambert, I.H., Simonsen, L.O. 1986. Separate, Ca^{2+}-activated K^+ and Cl^- transport pathways in Ehrlich ascites tumor cells. *J. Membrane Biol.* **91**:227–244

Hoffmann, E.K., Lambert, I.H., Simonsen, L.O. 1988. Mechanisms in volume regulation in Ehrlich ascites tumor cells. *Renal Physiol. Biochem.* **11**:221–247

Hoffmann, E.K., Simonsen, L.O. 1989. Membrane mechanisms in volume and pH regulation in vertebrate cells. *Physiol. Rev.* **69**:315–382

Hoffmann, E.K., Simonsen, L.O., Lambert, I.H. 1984. Volume-induced increase of K^+ and Cl^- permeabilities in Ehrlich ascites tumor cells. Role of internal Ca^{2+}. *J. Membrane Biol.* **78**:211–222

Hoffmann, E.K., Simonsen, L.O., Sjøholm, C. 1979. Membrane potential, chloride exchange, and chloride conductance in Ehrlich mouse ascites tumour cells. *J. Physiol.* **296**:61–84

Hoffmann, E.K., Ussing, H.H. 1992. Membrane mechanisms in volume regulation in vertebrate cells and epithelia. *In:* Membrane Transport in Biology. G.H. Giebisch, J.A. Schafer, H.H. Ussing, and P. Kristensen, editors. Vol. 5, pp. 317–399. Springer-Verlag, Heidelberg

Hudson, R.L., Schultz, S.G. 1988. Sodium-coupled glycine uptake by Ehrlich ascites tumor cells results in an increase in cell volume and plasma membrane channel activities. *Proc. Natl. Acad. Sci. USA* **85**:279–283

Jakobsen, K.B., Christensen O., Hoffmann, E.K. 1989. Ionic channels in Ehrlich ascites tumor cells. *Acta Physiol. Scand.* **136**:P9A

Kirber, M.T., Walsh, J.V., Singer, J.J. 1988. Stretch-activated ion channels in smooth muscle: A mechanism for the initiation of stretch-induced contraction. *Pfluegers Arch.* **412**:339–345

Kolb, H.-A., Ubl, J. 1987. Activation of anion channels by zymosan particles in membranes of peritoneal macrophages. *Biochim. Biophys. Acta.* **899**:239–246

Kramhøft, B., Lambert, I.H., Hoffmann, E.K., Jørgensen, F. 1986. Activation of Cl-dependent K transport in Ehrlich ascites tumor cells. *Am. J. Physiol.* **251**:C369–379

Kurtz, A. 1990. Do calcium-activated chloride channels control renin secretion. *NIPS* **5**:43–46

Lambert, I.H., Hoffmann, E.K., Jørgensen, F. 1989. Membrane

potential, anion and cation conductances in Ehrlich ascites tumor cells. *J. Membrane Biol.* **111:**113–132

Lansman, J.B., Hallam, T.J., Rink, T.J. 1987. Single stretch-activated ion channels in vascular endothelial cells as mechanotransducers? *Nature* **325:**811–813

Lewis, S.A., Donaldson, P. 1990. Ion channels and cell volume regulation: Chaos in an organized system. *News Physiol. Sci.* **5:**112–119

Li, M., McCann, J.D., Anderson, M.P., Clancy, J.P., Liedtke, C.M., Nairn, A.C., Greengard, P., Welsh, M.J. 1989. Regulation of chloride channel by protein kinase C in normal and cystic fibrosis airway epithelia. *Science* **244:**1353–1356

Marty, A., Tan, Y.P., Trautmann, A. 1984. Three types of calcium-dependent channels in rat lacrimal glands. *J. Physiol.* **257:**293–325

Moody, W.J., Bosma, M.M. 1989. A nonselective cation channel activated by membrane deformation in oocytes of the ascidian *Boltenia villosa*. *J. Membrane Biol.* **107:**179–188

Morris, C.E. 1990. Mechanosensitive ion channels. *J. Membrane Biol.* **113:**93–107

Okada, Y., Hazama, A. 1989. Volume-regulatory ion channels in epithelial cells. *News Physiol. Sci.* **4:**238–242

Okada, Y., Hazama, A., Yuan, W.L. 1990. Stretch-induced activation of Ca^{2+}-permeable ion channels is involved in the volume regulation of hypotonically swollen epithelial cells. *Neurosci. Res.* [*Suppl.*] **12:**S5–S13

Parent, L., Cardinal, J., Sauvé, R. 1988. Single-channel analysis of a K channel at basolateral membrane of rabbit proximal convoluted tubule. *Am. J. Physiol.* **254:**F1–F9

Pierce, S.K., Politis, A.D. 1990. Ca^{2+}-activated cell volume recovery mechanisms. *Annu. Rev. Physiol.* **52:**27–42

Rotin, D., Mason, M.J., Grinstein, S. 1991. Channels, antiporters, and regulation of cell volume in lymphoid cells. *In:* Advances in Comparative and Environmental Physiology. Vol. 9, Chap. 5. Springer-Verlag, Berlin—Heidelberg

Sachs, F. 1986. Biophysics of mechanoreception. *Membr. Biochem.* **6:**173–195

Sachs, F. 1987. Baroreceptor mechanisms at the cellular level. *Fed. Proc.* **46:**12–16

Sachs, F. 1988. Mechanical transduction in biological systems. *CRC Crit. Rev. Biomed. Eng.* **16:**141–169

Sackin, H. 1989. A stretch-activated K^+ channel sensitive to cell volume. *Proc. Natl. Acad. Sci. USA* **86:**1731–1735

Sauvé, R., Parent, L., Simoneau, C., Roy, G. 1988. External ATP triggers a biphasic activation process of a calcium-dependent K^+ channel in cultured bovine aortic endothelial cells. *Pfluegers Arch.* **412:**469–481

Sauvé, R., Simoneau, C., Monette, R., Roy, G. 1986. Single-channel analysis of the potassium permeability of HeLa cancer cells: Evidence for a calcium-activated potassium channel of small unitary conductance. *J. Membrane Biol.* **92:**269–282

Schultz, S.G. 1989. Intracellular sodium activities and basolateral membrane potassium conductances of sodium-absorbing epithelial cells. *In:* Cellular and Molecular Biology of Sodium Transport. S.G. Schultz, editor. *Curr. Top. Membr. Transp.* **34:**21–44

Spring, K.R., Hoffmann, E.K. 1991. Cellular volume control. *In:* The Kidney: Physiology and Pathophysiology. (2^{nd} ED.) D.W. Seldin and G. Giebisch, editors. Chap. 6, pp. 147–169. Raven, New York

Taglietti, V., Toselli, M. 1988. A study of stretch-activated channels in the membrane of frog oocytes: Interactions with Ca^{2+} ions. *J. Physiol.* **407:**311–328

Taniguchi, J., Guggino, W.B. 1989. Membrane stretch: A physiological stimulator of Ca^{2+}-activated K^+ channels in thick ascending limb. *Am. J. Physiol.* **257:**F347–F352

Ubl, J., Murer, H., Kolb, H.-A. 1988. Ion channels activated by osmotic and mechanical stress in membranes of opossum kidney cells. *J. Membrane Biol.* **104:**223–232

Welsh, M.J. 1986. An apical-membrane chloride channel in human tracheal epithelium. *Science* **232:**1648–1650

Yang, X.-C., Sachs, F. 1989. Block of stretch-activated ion channels in *Xenopus* oocytes by gadolinium and calcium ions. *Science* **243:**1068–1071

Received 7 August 1991; revised 23 January 1992